Stabilization of a Class of Large-Scale Systems of Linear Hyperbolic PDEs via Continuum Approximation of Exact Backstepping Kernels*

Jukka-Pekka Humaloja, *Member, IEEE*, and Nikolaos Bekiaris-Liberis, *Senior Member, IEEE*

***Abstract*— We establish that stabilization of a class of linear, hyperbolic partial differential equations (PDEs) with a large (nevertheless finite) number of components, can be achieved via employment of a backstepping-based control law, which is constructed for stabilization of a continuum version (i.e., as the number of components tends to infinity) of the PDE system. This is achieved by proving that the exact backstepping kernels, constructed for stabilization of the large-scale system, can be approximated (in certain sense such that exponential stability is preserved) by the backstepping kernels constructed for stabilization of a continuum version (essentially an infinite ensemble) of the original PDE system. The proof relies on construction of a convergent sequence of backstepping kernels that is defined such that each kernel matches the exact backstepping kernels (derived based on the original, large-scale system), in a piecewise constant manner with respect to an ensemble variable; while showing that they satisfy the continuum backstepping kernel equations. We present a numerical example that reveals that complexity of computation of stabilizing backstepping kernels may not scale with the number of components of the PDE state, when the kernels are constructed on the basis of the continuum version, in contrast to the case in which they are constructed on the basis of the original, large-scale system. In addition, we formally establish the connection between the solutions to the large-scale system and its continuum counterpart. Thus, this approach can be useful for design of computationally tractable, stabilizing backstepping-based control laws for large-scale PDE systems.**

***Index Terms*— Backstepping control, hyperbolic PDEs, large-scale systems, PDE continua.**

I. Introduction

A. Motivation

LARGE-SCALE systems of 1-D hyperbolic PDEs appear in a variety of applications involving transport phenomena and which incorporate different, interconnected components. Among them, large-scale interconnected hyperbolic systems may be used to describe the dynamics of blood flow, from the location of the heart all the way through to points where non-invasive measurements can be obtained [1], [2], of epidemics spreading, to describe transport of epidemics among different geographical regions [3], and of traffic flows, to model density and speed dynamics in interconnected highway segments [4], [5] and in urban networks [6], to name a few [7]. Backstepping is a systematic design approach to construction of explicit feedback laws for general classes of such systems [8]–[14]. Due to potentially large number of interacting components, incorporated in such systems, computational complexity of exact backstepping-based control designs may increase significantly, in a manner proportional with the number of state components. Motivated by this, in the present paper we aim at developing an approach to computing backstepping kernels for large-scale hyperbolic PDE systems, such that computational complexity remains tractable, even when the number of state components becomes very large, while at the same time, provably retaining the stability guarantees of backstepping. We achieve this via approximating the exact backstepping kernels, computed based on a large number of PDEs, utilizing a single kernel that is derived based on a continuum version of the exact kernels PDEs, and capitalizing on the robustness properties[1] of backstepping for the class of systems considered, to additive control gain errors.

*Funded by the European Union (ERC, C-NORA, 101088147). Views and opinions expressed are however those of the authors only and do not necessarily reflect those of the European Union or the European Research Council Executive Agency. Neither the European Union nor the granting authority can be held responsible for them.

[1]The authors are with the Department of Electrical and Computer Engineering, Technical University of Crete, Chania, Greece. Emails: jhumaloja@tuc.gr and nlimperis@tuc.gr.

B. Literature

The approach of design of feedback laws for large-scale systems based on a continuum version of the system considered has been utilized for large-scale ordinary differential equation (ODE) systems, such as, for example, in [16]–[23]. However, such an approach has not been utilized so far for large-scale systems whose state components are PDEs. The main goals of the approach developed here, may be viewed also as related to control design approaches that aim at providing computational means towards implementation of PDE backstepping-based control laws with provable stability guarantees, such as, for example, neural operators-based [24], late-lumping-based [25], and power series-based [26], backstepping control laws. Our approach may be viewed as complementary and different from these results, in that the main goal is to address

[1]Such robustness properties have been also reported within the framework of, e.g., robust output regulation for abstract, infinite-dimensional systems [15]. Thus, the approach presented here could be, in principle, also combined with other types of stabilizing feedback laws.

complexity due to a potential radical increase in the number of state components, instead of complexity of actual numerical implementation (even though these existing results can be combined with the approach presented here, for numerical implementation of the controllers).

C. Contributions

In the present paper, we provide backstepping-based feedback laws for a class of large-scale systems of 1-D hyperbolic PDEs, which are described by the class of systems considered in [13], when the number of state components n is large. The key idea of our approach is to construct approximate backstepping kernels for stabilization of the large-scale (nevertheless, with a finite number of components) system relying on the continuum backstepping kernels developed in [27] for a continuum version of the original, large-scale system. We establish stability of the closed-loop system consisting of the original, large-scale PDE system under a backstepping-based feedback law that employs the approximate kernels, constructed based on the continuum version of the PDE system. The stability proof consists of three main steps.

In the first, we construct a sequence of backstepping kernels that is defined such that each kernel matches with the exact backstepping kernel (derived based on the original, large-scale system) in a piecewise constant manner with respect to an ensemble variable; while showing that the kernels in the sequence satisfy the continuum kernel equation. For the proof we rely on a transformation that maps functions (the exact backstepping kernels) on a 2-D domain, to functions (the approximate kernels derived based on the continuum) on a 3-D domain in a piecewise constant manner in L^2 sense. In the second step, we show that this sequence converges to the continuum backstepping kernel, obtained from a direct application of backstepping to a continuum version of the large-scale system. For the proof we rely on the well-posedness of the backstepping kernels (both the continuum and exact kernels) and density arguments. In the third step, we establish stability of the closed-loop system employing an abstract systems framework. For the proof we recast the closed-loop system's dynamics as perturbed dynamics of the nominal (based on employment of the exact kernels) closed-loop system, showing that the size of the perturbation, due to the additive error that originates from the approximation error of the exact stabilizing control gains, can be made arbitrarily small (in L^2) for sufficiently large n.

We also provide an alternative stability proof employing a Lyapunov functional, which allows quantification of overshoot and decay rate of the closed-loop system's response. Furthermore, for enabling generalization of the approach introduced, for computation of stabilizing control gains based on continuum approximations, to other classes of large-scale PDE systems, we also establish the formal connection between the solutions to the original $n+1$ system and the solutions to its continuum counterpart. In particular, we show that when the number of state components is sufficiently large, the solutions to the large-scale system can be approximated by the solutions to the continuum system, provided that the data (i.e., parameters, initial conditions, and inputs) of the $n+1$ PDE problem can be approximated by the respective data of the continuum PDE problem. The proof relies on construction of a sequence of solutions, obtained in a piecewise constant manner (with respect to an ensemble variable) from the solutions to the $n+1$ system, which is subsequently shown (via utilization of the well-posedness property of the continuum that we prove) to converge to the solution of the continuum system.

We then present a numerical example that illustrates that computation of (approximate) stabilizing kernels based on the continuum kernel may provide flexibility in computation, as well as it may significantly improve computational complexity. In particular, in this specific example, although computation of the exact backstepping kernels may require to solve implicitly the corresponding $n+1$ hyperbolic kernels PDEs, as closed-form solutions may not be available, the approximate kernels can be computed with only algebraic computations, since the continuum kernel is available in closed form. We also present respective simulation investigations, which validate the theoretical developments, showing that as the number of components of the large-scale system increases the performance of the closed-loop systems, under the approximate control laws, is improved. In particular, we illustrate that the approximate control kernels converge to the exact kernels, and thus, as n increases, the performance of the closed-loop system becomes similar to the performance under the exact control gain kernels.

D. Organization

We start in Sections II and III presenting both the large-scale PDE system and its continuum counterpart, together with the respective exact and continuum backstepping kernels PDEs. In Section IV we establish stability of the large-scale, closed-loop system under the approximate control law. In Section V we present a numerical example and consistent simulation results. In Section VI we study the connection between the solutions to the large-scale system and its continuum counterpart. In Section VII we provide concluding remarks and discuss related topics of our current research.

E. Notation

We use the standard notation $L^2(\Omega;\mathbb{R})$ for real-valued Lebesgue integrable functions on an arbitrary domain Ω, and on one-dimensional domains H^1 denotes the corresponding Sobolev space. Similarly, $L^\infty(\Omega;\mathbb{R}), C(\Omega;\mathbb{R}), C^1(\Omega;\mathbb{R})$ denote essentially bounded, continuous, and continuously differentiable functions, respectively, on Ω. Moreover, $f \in L^2_{\text{loc}}([0,+\infty);\mathbb{R})$ means that $f \in L^2([0,m];\mathbb{R})$ for any $m \in \mathbb{N}$. We denote vectors and matrices by bold symbols, and $\|\cdot\|_\infty$ denotes the maximum absolute row sum of a matrix (or a vector). For any $n \in \mathbb{N}$, we denote by E the Hilbert space $L^2([0,1];\mathbb{R}^{n+1})$ equipped with the inner product

$$\left\langle \begin{pmatrix} \mathbf{u}_1 \\ v_1 \end{pmatrix}, \begin{pmatrix} \mathbf{u}_2 \\ v_2 \end{pmatrix} \right\rangle_E = \int_0^1 \left(\frac{1}{n} \sum_{i=1}^{n} u_1^i(x) u_2^i(x) + v_1(x) v_2(x) \right) dx, \quad (1)$$

which induces the norm $\|\cdot\|_E = \sqrt{\langle \cdot, \cdot \rangle_E}$. We also define the continuum version of E as $E_c = L^2([0,1];L^2([0,1];\mathbb{R})) \times$

$L^2([0,1];\mathbb{R})$, (i.e., $\mathbb{R}^n$ becomes $L^2([0,1];\mathbb{R})$ as $n\to\infty$) equipped with the inner product

$$\langle \left(\begin{smallmatrix} u_1 \\ v_1 \end{smallmatrix}\right), \left(\begin{smallmatrix} u_2 \\ v_2 \end{smallmatrix}\right) \rangle_{E_c} = \int_0^1 \left(\int_0^1 u_1(x,y)u_2(x,y)dy + v_1(x)v_2(x) \right) dx, \tag{2}$$

which coincides with $L^2([0,1]^2;\mathbb{R}) \times L^2([0,1];\mathbb{R})$. Moreover, $\mathcal{L}(E,\mathbb{R})$ denotes the space of bounded linear operators from E to $\mathbb{R}$, and $\|\cdot\|_{\mathcal{L}(E,\mathbb{R})}$ is the corresponding operator norm. For $\mathcal{L}(E,E)$, we denote $\mathcal{L}(E)$. Finally, we say that a system is exponentially stable (on E; resp. on E_c) if for any initial condition $z_0 \in E$ (resp. $z_0 \in E_c$) the (weak) solution $z(t)$ of the system satisfies $\|z(t)\|_E \le Me^{-ct}\|z_0\|_E$ (resp. $\|z(t)\|_{E_c} \le Me^{-ct}\|z_0\|_{E_c}$) for some $M, c > 0$ that are independent of z_0.

II. Stabilization of Large-Scale Systems of Linear Hyperbolic PDEs via Exact Backstepping Kernels

For $n \ge 1$ consider the following set of $n+1$ transport PDEs on $x \in [0,1]$ for $i = 1,\dots,n$

$$u_t^i(t,x) + \lambda_i(x)u_x^i(t,x) = \frac{1}{n}\sum_{j=1}^n \sigma_{i,j}(x)u^j(t,x) + W_i(x)v(t,x), \tag{3a}$$

$$v_t(t,x) - \mu(x)v_x(t,x) = \frac{1}{n}\sum_{j=1}^n \theta_j(x)u^j(t,x), \tag{3b}$$

with boundary conditions

$$u^i(t,0) = q_i v(t,0), \tag{4a}$$

$$v(t,1) = \frac{1}{n}\sum_{i=1}^n r_i u^i(t,1) + U(t), \tag{4b}$$

where $U \in L^2_{\text{loc}}([0,+\infty);\mathbb{R})$ is the control input. The initial conditions of (3) are $u^i(0,x) = u_0^i(x), v(0,x) = v_0(x)$, where $u_0^i, v_0 \in L^2([0,1];\mathbb{R})$. The parameters $\lambda_i, \mu, \sigma_{i,j}, W_i, \theta_i, q_i, r_i$ of the system (3), (4) satisfy the following assumption.

Assumption 2.1: We assume that $\mu, \lambda_i \in C^1([0,1];\mathbb{R})$, $\sigma_{i,j}, W_i, \theta_i \in C([0,1];\mathbb{R})$ and $q_i, r_i \in \mathbb{R}$ for all $i,j = 1,2,\dots,n$. Moreover, the transport velocities are assumed to satisfy $-\mu(x) < 0 < \lambda_i(x)$, for all $x \in [0,1]$ and $i = 1,2,\dots,n$.

Remark 2.2: The presentation of the system (3), (4) is motivated from [13]. However, here we also make the following modifications. Most notably, the factor $1/n$ appears in (3). This is equivalent to equipping the n-part of the system with the scaled inner product $n^{-1}\langle\cdot,\cdot\rangle_{\mathbb{R}^n}$. With the scaling, we guarantee that the sums remain bounded and convergent as $n\to\infty$ without having to pose any additional constraints on the parameters of (3), (4). If one wishes to proceed without scaling the sums, then some additional assumptions are needed, e.g., that the respective parameters form ℓ^p sequences for some $p \in [1,+\infty]$, such that the sums are well-defined as $n\to\infty$. The other noteworthy modification has to do with Assumption 2.1. In [13], the transport velocities are assumed to satisfy $-\mu(x) < 0 < \lambda_1(x) < \lambda_2(x) < \dots < \lambda_n(x), \forall x \in [0,1]$ to guarantee strict hyperbolicity and well-posedness of (3), (4)[2]. Nevertheless, well-posedness can be guaranteed under Assumption 2.1, e.g., based on [30, Sect. 13.2] as we show in Proposition A.1 in Appendix A. Due to well-posedness, the system (3), (4) has a well-defined, unique, weak solution $\left(\left(u^i(t,x)\right)_{i=1}^n, v(t,x)\right)$ on E, where $u^i, v \in C([0,+\infty);L^2([0,1];\mathbb{R}))$ [31, Prop. 4.2.5, Rem. 4.1.2].

It follows from [13, Thm 3.2] that the system (3), (4) is exponentially stabilizable by a state feedback law of the form

$$U(t) = -\frac{1}{n}\sum_{i=1}^n r_i u^i(t,1) + \int_0^1 \left[\frac{1}{n}\sum_{i=1}^n k^i(1,\xi)u^i(t,\xi) + k^{n+1}(1,\xi)v(t,\xi)\right] d\xi, \tag{5}$$

where, for $i = 1,\dots,n+1$, k^i satisfy

$$\mu(x)k_x^i(x,\xi) - \lambda_i(\xi)k_\xi^i(x,\xi) = \lambda_i'(\xi)k^i(x,\xi) + \frac{1}{n}\sum_{j=1}^n \sigma_{j,i}(\xi)k^j(x,\xi) + \theta_i(\xi)k^{n+1}(x,\xi), \tag{6a}$$

$$\mu(x)k_x^{n+1}(x,\xi) + \mu(\xi)k_\xi^{n+1}(x,\xi) = -\mu'(\xi)k^{n+1}(x,\xi) + \frac{1}{n}\sum_{j=1}^n W_j(\xi)k^j(x,\xi), \tag{6b}$$

on a triangular domain $0 \le \xi \le x \le 1$ with boundary conditions

$$k^i(x,x) = -\frac{\theta_i(x)}{\lambda_i(x)+\mu(x)}, \tag{7a}$$

$$\mu(0)k^{n+1}(x,0) = \frac{1}{n}\sum_{j=1}^n q_j\lambda_j(0)k^j(x,0), \tag{7b}$$

for all $x \in [0,1]$. Note the scaling of the sums by $1/n$ as per Remark 2.2.

III. Stabilization of a Continuum of Linear Hyperbolic PDEs via Continuum Backstepping

While large-scale, yet, consisting of a finite-number of components, systems of hyperbolic PDEs can be studied in the framework of Section II, we also consider the continuum limit case as $n\to\infty$, for which we present the generic framework of a continuum of hyperbolic PDEs studied in [27] and sketched in Fig. 1. That is, instead of having n rightward transport PDEs as in Section II, consider a continuum of such

[2] In specific cases, such an assumption may not be required, for example, for constructing a Lyapunov functional, see, e.g., [28], [29]. Moreover, differentiability of the transport velocities may not be needed in some cases, but here it guarantees the well-posedness of the kernel equations (6), (7).

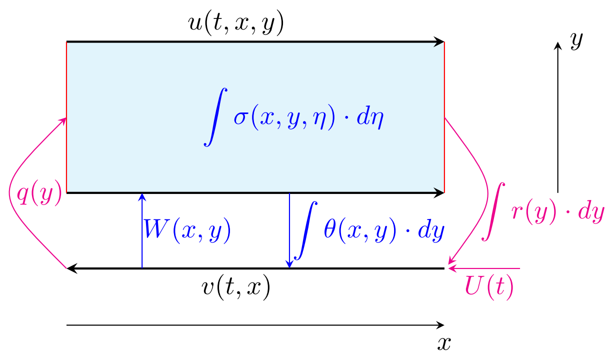

Fig. 1. Schematic view of the continuum PDE system (8), (9). Boundary terms are denoted in magenta and in-domain terms are denoted in blue.

PDEs as in [27] with $y \in [0,1]$ being the index variable[3]

$$u_t(t,x,y) + \lambda(x,y)u_x(t,x,y) = \int_0^1 \sigma(x,y,\eta)u(t,x,\eta)d\eta + W(x,y)v(t,x), \tag{8a}$$

$$v_t(t,x) - \mu(x)v_x(t,x) = \int_0^1 \theta(x,y)u(t,x,y)dy, \tag{8b}$$

with boundary conditions

$$u(t,0,y) = q(y)v(t,0), \tag{9a}$$

$$v(t,1) = \int_0^1 r(y)u(t,1,y)dy + U(t), \tag{9b}$$

for almost every $y \in [0,1]$, i.e., the continuum variables and parameters are considered $L^2([0,1];\mathbb{R})$ functions in y. The following assumption is needed, for the parameters involved in (8), (9), to guarantee the existence of a continuum backstepping control law [27, Thm 3].

Assumption 3.1: We assume that $\mu \in C^1([0,1];\mathbb{R}), \lambda \in C^1\left([0,1]^2;\mathbb{R}\right), W, \theta \in C([0,1];L^2([0,1];\mathbb{R})), \sigma \in C\left([0,1];L^2([0,1]^2;\mathbb{R})\right)$, and $q, r \in L^2([0,1];\mathbb{R})$. Moreover, $\lambda(x,y) > 0$ for all $x, y \in [0,1]$ and $-\mu(x) < 0$ for all $x \in [0,1]$.

By [27, Thm 1], the system (8), (9) is exponentially stabilizable by a state feedback law of the form

$$U(t) = -\int_0^1 r(y)u(t,1,y)dy + \int_0^1 \left[\int_0^1 k(1,\xi,y)u(t,\xi,y)dy + \bar{k}(1,\xi)v(t,\xi)\right] d\xi, \tag{10}$$

[3]Note that we have not yet formally proved that the continuum limit of system (3) as $n \to \infty$ is system (8). However, we use (8) here as an educated guess of such a continuum version (see also [27]) to obtain a continuum version of the respective backstepping kernels $k^i, i = 1, \ldots, n$, given in (6). In Section VI we, in fact, formally prove that (8), (9) is the continuum limit of (3), (4).

where $k, \bar{k}$ satisfy

$$\mu(x)k_x(x,\xi,y) - \lambda(\xi,y)k_\xi(x,\xi,y) - \theta(\xi,y)\bar{k}(x,\xi) = \lambda_\xi(\xi,y)k(x,\xi,y) + \int_0^1 \sigma(\xi,\eta,y)k(x,\xi,\eta)d\eta, \tag{11a}$$

$$\mu(x)\bar{k}_x(x,\xi) + \mu(\xi)\bar{k}_\xi(x,\xi) = -\mu'(\xi)\bar{k}(x,\xi) + \int_0^1 W(\xi,y)k(x,\xi,y)dy, \tag{11b}$$

on a triangular domain $0 \leq \xi \leq x \leq 1$ with boundary conditions

$$k(x,x,y) = -\frac{\theta(x,y)}{\lambda(x,y)+\mu(x)}, \tag{12a}$$

$$\mu(0)\bar{k}(x,0) = \int_0^1 q(y)\lambda(0,y)k(x,0,y)dy, \tag{12b}$$

for almost every $y \in [0,1]$.

IV. Stabilization of the Finite Large-Scale System via Continuum Approximation of Exact Kernels

A. Statement of the Main Result

The core idea of the continuum approximation that we present here is that we approximate $n+1$ kernel equations by a continuum of kernel equations. Provided that the approximation is sufficiently accurate, we show that the backstepping controller derived from the continuum kernel equations exponentially stabilizes the $n+1$ system associated with the original finite system of $n+1$ PDEs. We note that the kernel equations are independent of r_i (or r), and hence, this parameter is largely omitted in this section.

Thus, consider an $n+1$ system (3), (4) with parameters $\lambda_i, W_i, \theta_i, \sigma_{i,j}, q_i$ for $i, j = 1, 2, \ldots, n$ satisfying Assumption 2.1 and consider any continuous functions $\lambda, W, \theta, \sigma, q$ that satisfy Assumption 3.1 with

$$\lambda(x, i/n) = \lambda_i(x), \tag{13a}$$

$$W(x, i/n) = W_i(x), \tag{13b}$$

$$\theta(x, i/n) = \theta_i(x), \tag{13c}$$

$$\sigma(x, i/n, j/n) = \sigma_{i,j}(x), \tag{13d}$$

$$q(i/n) = q_i, \tag{13e}$$

for all $x \in [0,1]$ and $i, j = 1, 2, \ldots, n$. There are infinitely many functions satisfying (13) and Assumption 3.1, as well as ways to construct them, e.g., by utilizing auxiliary functions $\{p_i\}_{i=1}^n$ that satisfy $p_i(i/n) = 1$ and $p_\ell(i/n) = 0$ for $\ell \neq i$.[4]

[4]We demonstrate this by constructing $\sigma(x,y,\eta)$ satisfying (13d) of the form $\sigma(x,y,\eta) = \sum_{i=1}^n \sum_{j=1}^n \sigma_{i,j}(x)p_i(y)p_j(\eta)$, where

$$p_i(y) = \prod_{k=1,k\neq i}^n \frac{(k/n - y)}{(k/n - i/n)} + b\sin(n\pi y), \tag{14}$$

satisfies $p_i(i/n) = 1$, $p_\ell(i/n) = 0$ for $\ell \neq i$, and $p_i \in C^\infty([0,1];\mathbb{R})$ for any $i =, 1, 2, \ldots, n$ and any $b \in \mathbb{R}$. Similar constructions can be obtained for λ, W, θ, and q.

The relations in (13) could as well be defined in other ways, e.g., using $(i-1)/n$ in place of i/n, but we find (13) the most convenient option for our developments. The continuum kernel equations (11), (12) with parameters $\lambda, \mu, W, \theta, \sigma, q$, satisfying (13) and Assumption 3.1 have a unique, continuous solution $(k, \bar{k})$ by [27, Thm 3]. Thus, construct the following functions for all $0 \leq \xi \leq x \leq 1$[5]

$$\widetilde{k}^i(x,\xi) = n \int_{(i-1)/n}^{i/n} k(x,\xi,y)dy, \quad i = 1,2,\ldots,n, \tag{15a}$$

$$\widetilde{k}^{n+1}(x,\xi) = \bar{k}(x,\xi). \tag{15b}$$

Our main result is the following.

Theorem 4.1: Consider an $n+1$ system (3), (4) with parameters $\lambda_i, \mu, W_i, \theta_i, \sigma_{i,j}, q_i, r_i$ for $i,j = 1,2,\ldots,n$ satisfying Assumption 2.1. Let the parameters $\lambda, \mu, W, \theta, \sigma, q, r$ satisfy Assumption 3.1 and relations (13). Then, if n is sufficiently large, the system (3), (4) is exponentially stabilized by the control law

$$U(t) = -\frac{1}{n}\sum_{i=1}^{n} r_i u^i(t,1) + \int_0^1 \left[\frac{1}{n}\sum_{i=1}^{n} \widetilde{k}^i(1,\xi)u^i(t,\xi) + \widetilde{k}^{n+1}(1,\xi)v(t,\xi)\right] d\xi, \tag{16}$$

where $\left(\widetilde{k}^i\right)_{i=1}^{n+1}$ are given in (15), with $(k,\bar{k})$ being the solution to (11), (12).

B. Proof of Theorem 4.1

The proof of Theorem 4.1 relies on Lemmas 4.2 and 4.3 presented below. We show first that the functions defined in (15) approximate the solutions to the $n+1$ kernel equations (6), (7) to arbitrary accuracy as n increases. In order to do this, we first interpret the solutions to the $n+1$ kernels equations (6), (7) as piecewise constant solutions with respect to y, to the continuum kernels equations (11), (12). One way to do this is highlighted in the following lemma, which is to transform the $\mathbb{R}^n$-valued components of the $n+1$ kernel equations (6), (7) into step functions in $y \in [0,1]$.

Lemma 4.2: Consider the $n+1$ kernel equations (6), (7) where the parameters satisfy Assumption 2.1 and define the following functions for all $x \in [0,1]$, piecewise in y for $i,j = 1,2,\ldots,n$[6]

$$\lambda^n(x,y) = \lambda_i(x), \quad y \in (i-1)/n, i/n], \tag{17a}$$

$$\sigma^n(x,y,\eta) = \sigma_{i,j}(x), \quad y \in ((i-1)/n, i/n], \tag{17b}$$

$$\eta \in ((j-1)/n, j/n], \tag{17c}$$

$$W^n(x,y) = W_i(x), \quad y \in ((i-1)/n, i/n], \tag{17d}$$

$$\theta^n(x,y) = \theta_i(x), \quad y \in ((i-1)/n, i/n], \tag{17e}$$

$$q^n(y) = q_i, \quad y \in ((i-1)/n, i/n]. \tag{17f}$$

[5]If $k(x,\xi,\cdot)$ is continuous, one can instead define $\widetilde{k}^i(x,\xi) = k(x,\xi,i/n)$ for all $i = 1,\ldots,n$ and argue approximation accuracy based on continuity.

[6]These functions can be extended to $y \in [0,1]$ by assigning the value at $y = 0$ arbitrarily, which does not affect the functions in the L^2 sense. The same applies to (18).

Construct the following function for all $0 \leq \xi \leq x \leq 1$, piecewise in y for $i = 1,2,\ldots,n$

$$K^n(x,\xi,y) = k^i(x,\xi), \quad y \in ((i-1)/n, i/n], \tag{18}$$

where $\left(k^i\right)_{i=1}^{n+1}$ is the solution to (6), (7), and denote $\bar{K}^n = k^{n+1}$. Then, $\left(K^n, \bar{K}^n\right)$ satisfies the kernel equations (11), (12) for the parameters defined in (17) and the original μ.

Proof: The proof can be found in Appendix C.1. ■

Let us next consider the continuum of kernel equations (11), (12) with continuous parameters $\lambda, \mu, W, \theta, \sigma, q$ that satisfy (13) and Assumption 3.1, together with the respective kernel equations (11), (12) with piecewise constant parameters $\lambda^n, \mu, W^n, \theta^n, \sigma^n, q^n$ in y constructed in Lemma 4.2. In the next lemma, we show that the solution $\left(K^n, \bar{K}^n\right)$ to the latter approximates the solution $(k,\bar{k})$ to the former to arbitrary accuracy, provided that n is sufficiently large.

Lemma 4.3: Consider the solutions $\left(K^n, \bar{K}^n\right)$ to the kernel equations (11), (12) with parameters $\lambda^n, \mu, W^n, \theta^n, \sigma^n, q^n$ from Lemma 4.2. There exist continuous parameters $\lambda, \mu, W, \theta, \sigma, q$ constructed such that they satisfy Assumption 3.1 and (13), and for any such parameters the solution $(k,\bar{k})$ to the respective kernel equations (11), (12) exists and satisfies the following implications. For any $\delta > 0$, there exists an $n_\delta \in \mathbb{N}$ such that for all $n \geq n_\delta$ we have

$$\max_{(x,\xi)\in\mathcal{T}} \|k(x,\xi,\cdot) - K^n(x,\xi,\cdot)\|_{L^2([0,1];\mathbb{R})} \leq \delta, \tag{19a}$$

$$\max_{(x,\xi)\in\mathcal{T}} |\bar{k}(x,\xi) - \bar{K}^n(x,\xi)| \leq \delta, \tag{19b}$$

where we denote $\mathcal{T} = \{(x,\xi) \in [0,1]^2 : 0 \leq \xi \leq x \leq 1\}$.

Proof: The proof can be found in Appendix C.2. ■

Remark 4.4: The convergence of the solutions to the kernel equations (11), (12), with parameters $\lambda, \mu, W, \theta, \sigma, q$ holds true for any step functions that approximate the continuous parameters as in (C.10) and not only the ones defined in (17). Any such construction should be such that $\lambda^n, W, \theta^n, \sigma^n, q^n$ match with $\lambda, W, \theta, \sigma, q$ at some points in y within intervals of the form $[(i-1)/n, i/n]$.

We have by now established convergence of the solutions $\left(K^n, \bar{K}^n\right)$ to the kernel equations (11), (12) with parameters $\lambda^n, \mu, W^n, \theta^n, \sigma^n, q^n$ defined in (17), to the solutions $(k,\bar{k})$ to (11), (12) with parameters $\lambda, \mu, W, \theta, \sigma, q$. Since the solutions $\left(K^n, \bar{K}^n\right)$ are piecewise constant in y satisfying (18) and (19), where $\left(k^i\right)_{k=1}^{n+1}$ are the solutions to (6), (7) with parameters $\left(\lambda^i\right)_{i=1}^n, \mu, \left(W^i\right)_{i=1}^n, (\theta)_{i=1}^n, \left(q^i\right)_{i=1}^n$, the solutions $\left(K^n, \bar{K}^n\right)$ can, in fact, approximate the kernels $\left(k^i\right)_{i=1}^{n+1}$ to arbitrary accuracy as n gets sufficiently large. This in turn implies that the control law (16), constructed based on the solutions $(k,\bar{k})$ to the continuum kernel equations (11), (12), approximates (arbitrarily close as n gets sufficiently large) the original control law (5) constructed based on the solutions $\left(k^i\right)_{i=1}^{n+1}$ to the kernels equations (6), (7). For this, we present the following lemma.

Lemma 4.5: The control law (16) can be written as

$$\begin{aligned} U(t) = &-\frac{1}{n}\sum_{i=1}^{n} r_i u^i(t,1) \\ &+\int_0^1 \left(\frac{1}{n}\sum_{i=1}^{n} k^i(1,\xi)u^i(t,\xi) + k^{n+1}(1,\xi)v(t,\xi)\right) d\xi \\ &+\int_0^1 \left(\frac{1}{n}\sum_{i=1}^{n} \Delta k^i(1,\xi)u^i(t,\xi) + \Delta k^{n+1}(1,\xi)v(t,\xi)\right) d\xi, \end{aligned} \tag{20}$$

where $\left(k^i\right)_{i=1}^{n+1}$ is the solution to the $n+1$ kernel equations (6), (7), and the approximation error terms $\left(\Delta k^i(1,\cdot)\right)_{i=1}^{n+1}$ become arbitrarily small, uniformly in $\xi \in [0,1]$, when n is sufficiently large.

Proof: The proof can be found in Appendix C.3. ■

By Lemma 4.5, the control law (16) can be split into the part that exponentially stabilizes the large-scale $n+1$ system (3), (4) and to the Δ-part which we treat as a perturbation that becomes arbitrarily small when n is sufficiently large. Thus, the stability of the $n+1$ system under the control law (20) can be established based on existing results for well-posed infinite-dimensional linear systems. The well-posedness of the $n+1$ system and a generic stability result for perturbed well-posed linear systems are presented in Propositions A.1 and A.2, respectively, in Appendix A.

Proof of Theorem 4.1. As the term $-\frac{1}{n}\sum_{i=1}^{n} r_i u^i(t,1)$ in the control law (20) cancels out the boundary coupling in (4) at $x = 1$ in closed-loop, we consider the system (3), (4) with $r_i = 0$ for all $i = 1,\dots,n$ and the control law $\widetilde{U}(t) = U(t) + \frac{1}{n}\sum_{i=1}^{n} r_i u^i(t,1)$. By Proposition A.1 and [31, Sect. 10.1], we can translate the boundary-controlled PDE (3), (4) into a well-posed abstract Cauchy problem $\dot{z}(t) = Az(t) + B\widetilde{U}(t)$ on the Hilbert space E, where $z = (u^1,\dots,u^n,v)^T$, $\dot{z}(t) = Az(t)$ corresponds to (3) with the homogeneous boundary condition from (4) through the domain of A, and $B\widetilde{U}(t)$ corresponds to the boundary control in (4). Moreover, we introduce bounded linear operators K and ΔK corresponding to taking inner products (on E) with $\left(k^i(1,\cdot)\right)_{i=1}^{n+1}$ and $\left(\Delta k^i(1,\cdot)\right)_{i=1}^{n+1}$ such that the control law can be expressed as $\widetilde{U}(t) = Kz(t) + \Delta K z(t)$, where $\|\Delta K\|_{\mathcal{L}(E,\mathbb{R})} \le 2\delta + \varepsilon$ becomes arbitrarily small when n is sufficiently large by Lemma 4.5. Thus, the exponential stability of (3), (4) under the control law (20) follows from [13, Thm 3.2] and Proposition A.2. As this control law is equivalent to (16) by Lemma 4.5, this concludes the proof of Theorem 4.1.

Remark 4.6: The exponential stability of (3), (4) under the control law (20) can be alternatively shown using a Lyapunov functional, which can be found in Appendix C.4.

C. How Large n is Sufficiently Large?

In general, it is not possible to quantify (a priori), how large n needs to be in order for the approximate control law (16) to be exponentially stabilizing. This is because certain estimates generally tend to zero only asymptotically as n increases, such as the approximation of L^2 (or even generic continuous) functions by step functions in (C.10). However, under some additional smoothness assumptions on the parameters, it is possible to explicitly estimate the kernel approximation error and its decay rate as follows.

Proposition 4.7: Assume that the parameters of (6), (7) satisfy $\mu, \lambda_i \in C^2([0,1];\mathbb{R})$, $\sigma_{i,j}, W_i, \theta_i \in C^1([0,1];\mathbb{R})$ for all $i,j = 1,2,\dots,n$ along with Assumption 2.1. Construct respective Lipschitz-continuous (in y) continuum parameters of (11), (12) $\lambda \in C^2\left([0,1]^2;\mathbb{R}\right), W, \theta \in C^1([0,1];C([0,1];\mathbb{R})), \sigma \in C^1\left([0,1];C([0,1]^2;\mathbb{R})\right), q \in C([0,1];\mathbb{R})$ satisfying (13) and Assumption 3.1. Then, δ in (19) can be estimated by $\delta(n) = M_\delta/n$, where

$$\begin{aligned} M_\delta = M_L e^M \Bigg(&\frac{M_q}{m_\mu} + 2M_q M'_\lambda \bar{\phi}' e^{\bar{M}'_1} \\ &+ \left(\frac{M_q}{m_\mu} + 6M_q + \frac{M_b}{m_\mu} + 2\right)\bar{\phi} e^{\bar{M}_1}\Bigg), \end{aligned} \tag{21}$$

where M_L denotes the maximum over the Lipschitz constants in y of the continuum parameters,

$$m_\lambda = \min_{(x,y)\in[0,1]^2} \lambda(x,y), \quad m_\mu = \min_{x\in[0,1]} \mu(x), \tag{22a}$$

$$M'_\lambda = \max_{(x,y)\in[0,1]^2} |\lambda_x(x,y)|, \quad M'_\mu = \max_{x\in[0,1]} |\mu'(x)|, \tag{22b}$$

$$M_q = 1 + \frac{\|\lambda(0,\cdot)\|_{L^\infty([0,1];\mathbb{R})}}{m_\mu}\|q\|_{L^\infty([0,1];\mathbb{R})}, \tag{22c}$$

$$M_b = M_L + \|\lambda(0,\cdot)\|_{L^\infty([0,1];\mathbb{R})} + \|q\|_{L^\infty([0,1];\mathbb{R})}, \tag{22d}$$

$$\begin{aligned} M = &\frac{M_q}{m_\lambda}\left(M'_\lambda + \max_{x\in[0,1]}\left\|\int_0^1 \sigma(x,\cdot,\eta)d\eta\right\|_{L^\infty([0,1];\mathbb{R})}\right) \\ &+ \frac{M_q}{m_\lambda}\max_{x\in[0,1]}\|\theta(x,\cdot)\|_{L^\infty([0,1];\mathbb{R})} \\ &+ \frac{M'_\mu + \max_{x\in[0,1]}\|W(x,\cdot)\|_{L^\infty([0,1];\mathbb{R})}}{m_\mu}, \end{aligned} \tag{22e}$$

and $\bar{\phi}, \bar{\phi}', \bar{M}_1, \bar{M}'_1$ are such that

$$\sup_{n\in\mathbb{N}}\max_{(x,\xi)\in\mathcal{T}} \|K^n(x,\xi,\cdot)\|_{L^2([0,1];\mathbb{R})} \le \bar{\phi} e^{\bar{M}_1}, \tag{23a}$$

$$\sup_{n\in\mathbb{N}}\max_{(x,\xi)\in\mathcal{T}} |\bar{K}^n(x,\xi,\cdot)| \le \bar{\phi} e^{\bar{M}_1}, \tag{23b}$$

$$\sup_{n\in\mathbb{N}}\max_{(x,\xi)\in\mathcal{T}} \|K^n_\xi(x,\xi,\cdot)\|_{L^2([0,1];\mathbb{R})} \le \bar{\phi}' e^{\bar{M}'_1}. \tag{23c}$$

Proof: The proof can be found in Appendix C.5. ■

V. Numerical Example

A. Stabilization via Approximate Kernels

As an example, consider an $n+1$ system (3), (4) with parameters $\mu(x) = 1$ and

$$\lambda_i(x) = 1, \tag{24a}$$

$$\sigma_{i,j}(x) = x^3(x+1)\left(\frac{i}{n} - \frac{1}{2}\right)\left(\frac{j}{n} - \frac{1}{2}\right), \tag{24b}$$

$$W_i(x) = x(x+1)e^x\left(\frac{i}{n} - \frac{1}{2}\right), \tag{24c}$$

$$\theta_i(x) = -70e^{x\frac{35}{\pi^2}}\frac{i}{n}\left(\frac{i}{n} - 1\right), \tag{24d}$$

$$q_i = \cos\left(2\pi\frac{i}{n}\right), \qquad r_i = 0, \tag{24e}$$

for $i, j = 1, \dots, n$ such that continuous functions satisfying (13) can be constructed as $\lambda(x, y) = 1$ and

$$\sigma(x, y, \eta) = x^3(x+1)\left(y - \frac{1}{2}\right)\left(\eta - \frac{1}{2}\right), \tag{25a}$$

$$W(x, y) = x(x+1)e^x\left(y - \frac{1}{2}\right), \tag{25b}$$

$$\theta(x, y) = -70e^{x\frac{35}{\pi^2}} y\,(y-1)\,, \tag{25c}$$

$$q(y) = \cos(2\pi y). \tag{25d}$$

The latter parameter values correspond to the example considered in [27, Sect. VII], where it is shown that the solutions of the corresponding continuum kernel equations are given by

$$k(x, \xi, y) = 35y(y-1)e^{2\xi \bar{k}(x,\xi)}, \quad \bar{k}(x, \xi) = \frac{35}{2\pi^2}. \tag{26}$$

We note that while a closed-form solution exists to the continuum kernel equations (11), (12) with parameters (25), we were not able to solve the corresponding $n+1$ kernel equations (6), (7) with parameters (24) in closed-form when $n \in \mathbb{N}$ is arbitrary, nor do we expect that a closed-form solution can be constructed (even for small n). This is also consistent with, e.g., [32], in which an explicit solution is possible to obtain for the specific case $n = 1$ and for spatially invariant parameters (24). Regardless, in this particular example, the continuum approximation significantly simplifies the computation of the stabilizing control kernels.

We simulate the $n+1$ system (3), (4) with parameters (24) under the control law (16) computed based on the continuum kernels (26). Various values of n are considered to illustrate the behavior of the closed-loop system as n increases. In fact, the closed-loop system is stable for any $n \geq 2$, but the performance is improved for larger n. However, when $n = 1$, the system (3), (4) is open-loop stable and $k^1(x, \xi) = k^2(x, \xi) = 0$ is the solution to the kernel equations (6), (7), in which case the approximate control law (16) destabilizes the system (because $\bar{k} \neq 0$, in contrast to k^2).

In the simulations, the system (3), (4) is approximated using finite differences with 256 grid points in $x \in [0, 1]$. The ODE resulting from the finite-difference approximation is solved using `ode45` in MATLAB. The initial conditions for all n are $u_0^i(x) = q_i$ for $i = 1, \dots, n$ and $v_0(x) = 1$, for all $x \in [0, 1]$. Fig. 2 displays the control law (16) when $n = 2, \dots, 6$. We note that the control law also acts as a weighted average of the solution to (3), (4), i.e., we can also assess the exponential decay rate of the solutions based on $U(t)$. However, as $k(x, \xi, 1) = 0$ in (26), the component $u^n(t, x)$ does not affect the control in any way. Therefore, $u^n(t, x)$ is displayed separately in Fig. 3 for $n = 2, \dots, 5$, which shows that also $u^n(t, x)$ decays to zero as $t \to \infty$.

Fig. 2 and Fig. 3 show that the approximate control law based on the continuum kernels (26) is indeed stabilizing already when $n = 2$, even if the rate of decay is very slow. However, Fig. 2 and Fig. 3 show that the closed-loop performance significantly improves when n becomes larger, and in Fig. 2 the controls for $n = 5$ and $n = 6$ are virtually indistinguishable. Later on in Fig. 4, we see that the controls do still change slightly, e.g., for $n = 10$, but regardless, the

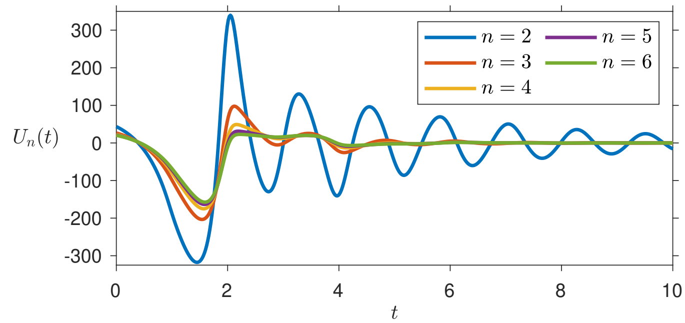

Fig. 2. The controls $\boldsymbol{U(t)}$ based on the approximate control law (16) when $\boldsymbol{n = 2, \dots, 6}$.

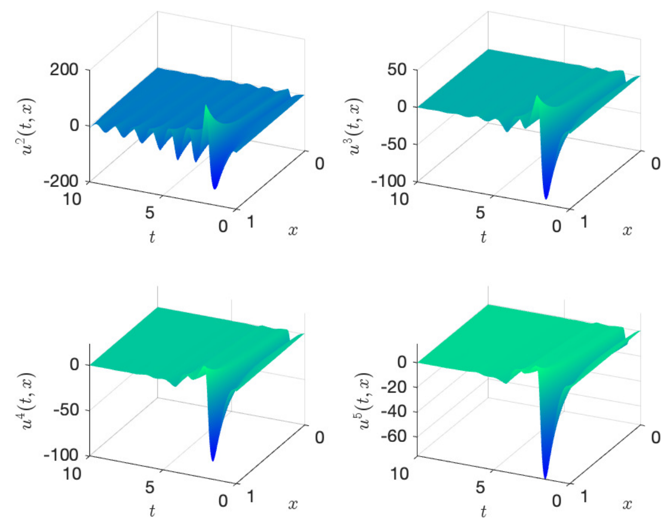

Fig. 3. The solution component $\boldsymbol{u^n(t, x)}$ when $\boldsymbol{n = 2, \dots, 5}$.

controls, along with the solutions, have practically converged to zero by $t = 6$ already for $n = 6$. We note that it takes the control input $1/\mu + 1/\lambda = 2$ time units to traverse through the system (3), (4) for any n, which is why, e.g., the state component $u^n(t, \xi)$, may grow rapidly in the beginning of the simulation, as seen in Fig. 3 before getting stabilized by the controls. However, due to the in-domain coupling between u and v in (3), the controls do affect the u^i components through v already before entering the u^i channels at time $t = 1/\mu = 1$.

The simulations demonstrate that the approximate control law (16) based on the continuum kernels (26) exponentially stabilizes the $n+1$ system (3), (4) when n is sufficiently large, and that the approximation error of the control law decreases as n increases. Thus, the simulations are well in accordance with the theoretical results. Moreover, in this example, the approximate control law has good performance already for very moderate n, showing that the sufficiently large n appearing in the theoretical results may be, in practice, relatively small. However, one should not expect this to be the case in general, as this is dependent on the parameters of both the system (3), (4) and its continuum approximation (8), (9).

B. Comparison with Exact Controls

In this subsection, we compare the performance of the closed-loop systems under the approximate and exact kernels. However, as we are not aware of the existence of closed-form solutions to (6), (7), we have to find the solution implicitly, and hence, the presented comparisons are between the closed-form continuum kernels (26) and numerical approximations of the exact kernels obtained from (6), (7). Regardless, we refer to the numerical solution to (6), (7) as the exact kernels. We note that, consistently with the number of exact kernels, the computational burden of solving (6), (7) appears to grow (roughly linearly) with n. For example, for $n = 3, 5, 10, 20$, it took $14.3, 15.2, 17.7$, and 21.4 seconds[7], respectively, to solve the exact $n + 1$ kernels. On the other hand, computing the approximate kernels is virtually invariant to n, as such computations rely only on evaluation of $k(1, \xi, y)$ given in (26) at the given points in y.

In Fig. 4, we compare the control efforts obtained by using the approximate continuum kernels and the exact kernels obtained from (6), (7) for $n = 3, 5, 10, 20$. It can be seen that qualitatively the controls computed based on the exact kernels seem to behave the same despite of n. Moreover, as expected from Fig. 2, the approximate control laws computed based on the continuum kernels (26) get closer to the exact controls as n increases. Regardless, it can be seen from Fig. 4 that the differences in closed-loop performance are small already at $n = 10$.

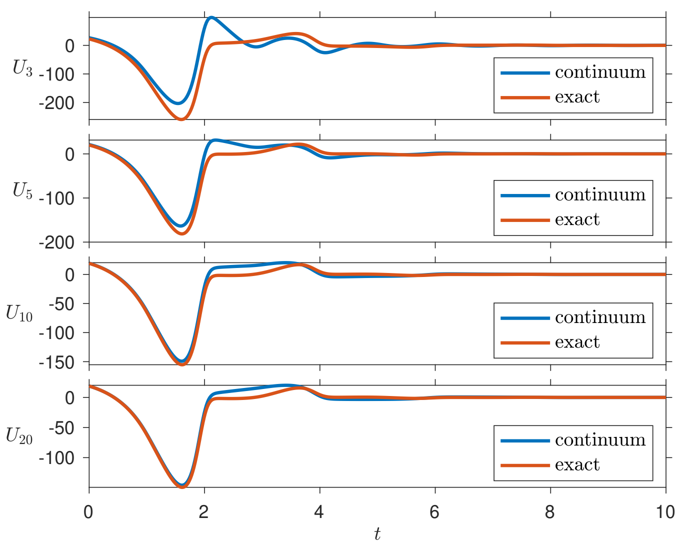

Fig. 4. Comparison of the control efforts with the continuum (approximate) kernels and the exact control kernels for $n = 3, 5, 10, 20$.

VI. Approximation of the Solutions to the Large-Scale System by a Continuum

In this section, we show that the continuum system (8), (9) acts as an approximation of the $n+1$ system (3), (4), when n is sufficiently large. In particular, a sequence of solutions to (3), (4) can approximate the solution to (8), (9), provided that the sequence of data of (3), (4) approximates the data of (8), (9) (including initial conditions) to arbitrary accuracy.

Theorem 6.1: Consider an $n + 1$ system (3), (4), with parameters $\lambda_i, \mu, W_i, \theta_i, \sigma_{i,j}, q_i, r_i$ for $i, j = 1, 2, \ldots, n$ satisfying Assumption 2.1, initial conditions $v_0, u_0^i \in L^2([0, 1]; \mathbb{R})$ for $i = 1, 2, \ldots, n$, and input $U \in L^2_{\text{loc}}([0, +\infty); \mathbb{R})$. Construct a continuum system (8), (9), with parameters $\lambda, \mu, W, \theta, \sigma, q, r$ that satisfy Assumption 3.1, (13), and with $r \in C([0, 1]; \mathbb{R})$ satisfying[8]

$$r(i/n) = r_i, \qquad i = 1, 2, \ldots, n. \tag{27}$$

Moreover, equip (8), (9) with initial conditions u_0, v_0 and input U, such that u_0 is continuous in y and satisfies

$$u_0(x, i/n) = u_0^i(x), \tag{28}$$

for $i = 1, 2, \ldots, n$[9]. Sample the solution (u, v) to the resulting PDE system (8), (9) for these data, into a vector-valued function $((\tilde{u}_i)_{i=1}^n, \tilde{v})$ as $\tilde{\mathbf{u}}(t, x) = \mathcal{F}_n^* u(t, x, \cdot)$[10] and $\tilde{v}(t, x) = v(t, x)$, pointwise for all $t \geq 0$ and almost all $x \in [0, 1]$. On any compact interval $t \in [0, T]$, for any given $T > 0$, we have

$$\max_{t \in [0,T]} \left\| \begin{pmatrix} \mathbf{u}(t) \\ v(t) \end{pmatrix} - \begin{pmatrix} \tilde{\mathbf{u}}(t) \\ \tilde{v}(t) \end{pmatrix} \right\|_E \leq \delta_2 + \varepsilon_2 + \delta_3 + \varepsilon_3, \tag{29}$$

where $\varepsilon_2, \varepsilon_3, \delta_2, \delta_3 > 0$ become arbitrarily small when n is sufficiently large.

Proof: The proof can be found in Appendix C.6. ■

Remark 6.2: The conclusion of Theorem 6.1 remains valid even if the input U was not exactly the same for both PDE systems. That is, rewriting (C.43) with U replaced by some $\bar{U}$ in (C.40) results in an additional error term $\|\Phi_t\|_{\mathcal{L}(L^2([0,T];\mathbb{R});E_c)} \|U - \bar{U}\|_{L^2([0,T],\mathbb{R})}$, which can be made arbitrarily small by assuming $\|U - \bar{U}\|_{L^2([0,T],\mathbb{R})}$ is sufficiently small, since the operator norm of Φ_t is uniformly bounded on compact intervals $t \in [0, T]$ (based on Proposition B.1 in Appendix B).

VII. Conclusions and Discussion

Computation of approximate stabilizing kernels based on the continuum kernel may provide flexibility in computation (also in terms of the number of different kernels being computed), as well as it may significantly improve computational complexity (although, practically, such computation also depends on the sampling method chosen for the continuum kernel). This is confirmed in the numerical example in which computational burden of stabilizing kernels is significantly improved, since the approximate kernels computed based on the continuum can be computed in closed form, in contrast to the exact kernels that have to be computed implicitly based on the solution to the kernel PDEs.

In general, we may expect that the complexity of computation of stabilizing control gains via the continuum approximation approach to not scale with n, i.e., to be $\mathcal{O}(1)$; while the complexity of computation of the exact control kernels to be

[7]Computed based on finite differences in MATLAB 2023b on a 2023 MacBook Pro with Apple M3 chip and 8 GB of memory.

[8]Continuity of r is only assumed for (27) to be well-defined; generally $r \in L^2([0, 1]; \mathbb{R})$ is sufficient for the continuum parameter.

[9]Such functions can always be constructed as, e.g., per Footnote 4.

[10]The transform $\mathcal{F}_n$ is introduced in the proof of Lemma 4.2, and its adjoint $\mathcal{F}_n^*$ satisfies (C.5).

$\mathcal{O}(n)$, i.e., to grow with the number of state components. Thus, this approach may be useful for computationally efficient control of large-scale PDE systems. This is confirmed in [33], where, in addition, we have identified a class of continuum systems for which a closed-form solution to the respective continuum kernel equations can be obtained.

Although in Section IV-C we provide, under additional conditions on the parameters, an explicit estimate of the kernels approximation error as function of n, in practice, such estimates may be conservative. For this reason, developing constructive methods for finding optimal (in certain sense) continuum approximations for a given $n+1$ system is an important research direction. We have made a first step towards this direction in [33] relying on polynomial approximations of the continuum parameters and using power series to compute the continuum kernels. Another important usage of the approach presented may be in designing observer-based, output-feedback controllers for large-scale $n+1$ hyperbolic PDEs, where the control gain may be constructed based on the proposed continuum approximation and Theorem 6.1 may be utilized in construction of approximate continuum observers. Moreover, although the present paper focuses on development of fundamental results, application of our theory to a practically relevant engineering system, such as, for example, to control of multi-lane or multi-class traffic flows [34, Ch. 8–9], would be significant, and thus, it could be pursued as topic of future research.

APPENDIX

A. Technical Propositions

This appendix contains two technical results regarding the well-posedness of the $n+1$ system (3), (4) under Assumption 2.1, and a generic result regarding exponential stability of perturbed, well-posed, infinite-dimensional linear systems. Both results are direct consequences of existing results in the literature.

Proposition A.1: The system (3), (4) is well-posed on $L^2([0,1];\mathbb{R}^{n+1})$ for any parameters satisfying Assumption 2.1.

Proof: We utilize [30, Thm 13.2.2], for which we need to show that the system (3), (4) can be interpreted as a port-Hamiltonian system satisfying the assumptions of this theorem. Thus, we write the system (3) in the form $z_t(t,x) = P_1(\mathcal{H}(x)z(t,x))_x + D(x)z(t,x)$, where $z = (u^1,\dots,u^n,v)^T, P_1 = \mathrm{diag}(-I_{n\times n},1) = P_1^T, \mathcal{H} = \mathrm{diag}(\lambda_1,\dots,\lambda_n,\mu) \in C^1([0,1];\mathbb{R}^{(n+1)\times(n+1)})$ by Assumption 2.1 and D is a bounded linear operator. More precisely, $D = -P_1\mathcal{H}' + D_1$, where D_1 is such that $D_1(x)z(x,t)$ corresponds to the right-hand-side of (3), and the the diagonal operator $P_1\mathcal{H}$ satisfies the first assumption of [30, Thm 13.2.2] by Assumption 2.1.

For the boundary conditions (4), we define a vector $f = (u^1(0),\dots,u^n(0),\, v(0), u^1(1),\dots,u^n(1),v(1))^T$ comprising the boundary values of z. Using this, the boundary condition $u^i(\cdot,0) = q_i v(\cdot,0)$ can be written as $W_{B,1}f = 0$, where $W_{B,1} = \begin{bmatrix} I_{n\times n} & -\mathbf{q} & 0_{n\times(n+1)}\end{bmatrix}$, where we denote $\mathbf{q} = (q_1,\dots,q_n)^T$. The boundary condition $v(\cdot,1) = \frac{1}{n}\sum_{i=1}^n r_i u^i(t,1) + U(\cdot)$ can be written as $W_{B,2}f = U$, where $W_{B,2} = \begin{bmatrix} 0_{1\times(n+1)} & -\frac{\mathbf{r}}{n} & 1\end{bmatrix}$, where we denote $\mathbf{r} = (r_1,\dots,r_n)^T$. Thus, the matrix $W_B = \begin{bmatrix} W_{B,1} \\ W_{B,2}\end{bmatrix}$ has full rank regardless of $\mathbf{q}$ and $\mathbf{r}$, which covers the second assumption of [30, Thm 13.2.2]. Thus, by [30, Thm 13.2.2, Rem. 13.2.3], the system (3), (4) is well-posed. ■

Proposition A.2: Consider a well-posed abstract Cauchy problem $\dot{z}(t) = Ax(t) + BU(t)$ on a Hilbert space Z under feedback control law $U(t) = (K+\Delta K)z(t)$, where K and ΔK are bounded linear operators. If the feedback law $U(t) = Kz(t)$ is exponentially stabilizing, then so is $U(t) = Kz(t) + \Delta K z(t)$, provided that $\|\Delta K\|_{\mathcal{L}(Z,\mathbb{R})}$ is sufficiently small.

Proof: The proof relies on the well-posedness of the abstract Cauchy problem, i.e., B being an admissible control operator for (the strongly continuous semigroup generated by) A [31, Sect. 4.2], and the Gearhart-Greiner-Prüss Theorem [35, Thm V.1.11]. Let us denote $A_K = A + BK$ which is the generator of an exponentially stable semigroup on Z, i.e., the solution to $\dot{z}(t) = (A+BK)z(t), z(0) = z_0$ satisfies $\|z(t)\|_Z \le Me^{-\gamma t}\|z_0\|_Z$ for some $M,\gamma > 0$. Now, the system under the perturbed control law can be written as $\dot{z}(t) = A_K z(t) + B\Delta K z(t)$, where B is admissible for A_K by [31, Cor. 5.5.1]. Moreover, there exists some $K_{\gamma/4} > 0$ such that [31, Prop. 4.4.6]

$$\begin{aligned}\|(sI - A_K)^{-1}B\Delta K\|_{\mathcal{L}(Z)} &\le \frac{K_{\gamma/4}}{\sqrt{\mathrm{Re(s)}+\gamma/4}}\|\Delta K\|_{\mathcal{L}(Z,\mathbb{R})}, \quad \forall \mathrm{Re}(s) > -\gamma/4 \\ &\le \frac{2K_{\gamma/4}}{\sqrt{\gamma}}\|\Delta K\|_{\mathcal{L}(Z,\mathbb{R})}, \quad \forall \mathrm{Re}(s) > 0, \end{aligned} \tag{A.1}$$

where, in place of $-\gamma/4$ we could use any value on $(-\gamma,0)$.

The rest of the proof utilizes spectral arguments. Based on the identity $(sI - A_K - B\Delta K) = (sI - A_K)(I + (sI - A_K)^{-1}B\Delta K)$, we see that any point $s\in\mathbb{C}$ is guaranteed to be in the resolvent set of $A_K + B\Delta K$ if it is in the resolvent set of A_K and $\|(sI - A_K)^{-1}B\Delta K\|_{\mathcal{L}(Z)} < 1$. By the exponential stability of A_K and (A.1), these conditions can be guaranteed for all $\mathrm{Re(s)} > 0$ when $\|\Delta K\|_{\mathcal{L}(Z,\mathbb{R})}$ is sufficiently small, in addition to the resolvent operator $(sI - A_K - B\Delta K)^{-1}$ being uniformly bounded for all $\mathrm{Re(s)} > 0$. Thus, for $\|\Delta K\|_{\mathcal{L}(Z,\mathbb{R})}$ sufficiently small, we have that $A_K + B\Delta K$ is exponentially stable by [35, Thm V.1.11], which concludes the proof. ■

B. Well-Posedness of the Continuum System

The following proposition states the well-posedness result for (8), (9), analogously to what has been stated in Proposition A.1 for (3), (4).

Proposition B.1: The continuum system (8), (9) is well-posed on $E_c = L^2([0,1];L^2([0,1];\mathbb{R}))\times L^2([0,1];\mathbb{R})$ for any parameters satisfying Assumption 3.1. That is, for any initial conditions $u_0 \in L^2([0,1];L^2([0,1];\mathbb{R})), v_0 \in L^2([0,1];\mathbb{R})$ and input $U \in L^2_{\mathrm{loc}}([0,+\infty);\mathbb{R})$, there is a unique (weak) solution to (8), (9) satisfying $(u,v)\in C([0,+\infty);E_c)$.

Proof: In order to show the well-posedness of the continuum system (8), (9), due to [30, Lem. 13.1.14], we only need to show the well-posedness of the pure transport part, i.e.,

$$u_t(t,x,y) + \lambda(x,y)u_x(t,x,y) = 0, \tag{B.1a}$$
$$v_t(t,x) - \mu(x)v_x(t,x) = 0, \tag{B.1b}$$

with boundary conditions (9) and initial conditions $u(0,x,y) = u_0(x,y), v(0,x) = v_0(x)$. Moreover, we first consider the case $r = 0$ and then employ [30, Thm 13.1.12] for $r \neq 0$. For now, assuming that everything is sufficiently smooth, the solution to (B.1), (9) for $r = 0$ is (cf. [36, Prop. 3.1])

$$v(t,x) = \begin{cases} v_0\left(\phi_\mu^{-1}(\phi_\mu(x)+t)\right), & t - \int_x^1 \frac{d\xi}{\mu(\xi)} \leq 0 \\ U\left(t - \int_x^1 \frac{d\xi}{\mu(\xi)}\right), & t - \int_x^1 \frac{d\xi}{\mu(\xi)} > 0 \end{cases}, \tag{B.2a}$$

$$u(t,x,y) = \begin{cases} u_0\left(\phi_{\lambda_y}^{-1}(\phi_{\lambda_y}(x)-t), y\right), & t - \int_0^x \frac{d\xi}{\lambda(\xi,y)} \leq 0 \\ q(y)v\left(t - \int_0^x \frac{d\xi}{\lambda(\xi,y)}, 0\right), & t - \int_0^x \frac{d\xi}{\lambda(\xi,y)} > 0 \end{cases}, \tag{B.2b}$$

where $\phi_\mu(x) = \int_0^x \frac{d\xi}{\mu(\xi)}$ and $\phi_{\lambda_y}(x) = \int_0^x \frac{d\xi}{\lambda(\xi,y)}$, pointwise for (almost) every $y \in [0,1]$. The solution (B.2) is well-defined, unique, and depends continuously on λ, μ, v_0, u_0 and U. The solution formula (and thus, the properties of the solution) is valid for any $v_0 \in H^1([0,1];\mathbb{R}), u_0 \in H^1([0,1]; L^2([0,1];\mathbb{R}))$, and $U \in H^1_{\text{loc}}([0,+\infty);\mathbb{R})$ under the compatibility conditions $v_0(1) = U(0)$ and $u_0(0,y) = q(y)v_0(0)$, i.e., (B.2) is the classical solution of (B.1). Moreover, for any $v_0 \in L^2([0,1];\mathbb{R}), u_0 \in L^2([0,1]; L^2([0,1];\mathbb{R}))$ and $U \in L^2_{\text{loc}}([0,+\infty);\mathbb{R})$, we can construct a unique weak solution as the limit of a sequence of classical solutions [7, Sect. 2.1.3] due to H^1 being dense in L^2 (on one-dimensional intervals) by the Sobolev Embedding Theorem. Thus, the system (B.1), (9) for $r = 0$ is well-posed on $L^2([0,1]; L^2([0,1];\mathbb{R})) \times L^2([0,1];\mathbb{R})$.

For $r \neq 0$, we employ [30, Thm 13.1.12] and view the boundary coupling at $x = 1$ as an output feedback connection. Thus, defining the auxiliary output as $Y_{\text{a}}(t) = \int_0^1 r(y)u(t,1,y)dy$, the system (B.1), (9) is well-posed if the inverse of $1 - G(s)$ exists and is boundedly invertible for all $s \in \mathbb{C}$ with $\text{Re}(s)$ sufficiently large, where G denotes the transfer function from U to Y_{a} for $r = 0$. By [37, Thm 2.9], $G(s)$ can be computed from

$$su(s,x,y) + \lambda(x,y)u_x(s,x,y) = 0, \tag{B.3a}$$
$$sv(s,x) + \mu(x)v_x(s,x) = 0, \tag{B.3b}$$
$$u(s,0,y) = q(y)v(s,0), \tag{B.3c}$$
$$v(s,1) = U(s), \tag{B.3d}$$
$$\int_0^1 r(y)u(s,1,y)dy = Y_{\text{a}}(s), \tag{B.3e}$$

where $Y_{\text{a}}(s) = G(s)U(s)$. Solving (B.3) gives

$$G(s) = \int_0^1 r(y)q(y)\exp\left(-s\int_0^1 \lambda(\zeta,y)d\zeta\right)dy \times \exp\left(-s\int_0^1 \mu(\zeta)d\zeta\right). \tag{B.4}$$

Thus, due to $\mu, \lambda > 0$ by Assumption 3.1, we have that $\text{Re}\,(G(s)) \to 0$ as $\text{Re}(s) \to +\infty$, and hence, (B.1), (9) is well-posed by [30, Thm 13.1.12]. Finally, since (8), (9) only differs from (B.1), (9) by a bounded additive perturbation (i.e., everything on the right-hand side of (8)), we have that (8), (9) is well-posed by [30, Lem. 13.1.14]. ■

C. Proofs for Sections IV and VI

1) Proof of Lemma 4.2: The claim follows after applying a linear transform to the kernel equations (6), (7). In order to rigorously present the transformation, we have to write (6) as a single equation on $\mathbb{R}^{n+1}$. We introduce the following notation

$$\mathbf{k}(x,\xi) = \left(k^i(x,\xi)\right)_{i=1}^{n+1}, \tag{C.1a}$$
$$\mathbf{L}(x) = \text{diag}\left(\left(\lambda^i(x)\right)_{i=1}^n, -\mu(x)\right), \tag{C.1b}$$
$$\mathbf{S}(x) = \frac{1}{n}\begin{bmatrix} \sigma_{1,1}(x) & \cdots & \sigma_{n,1}(x) & n\theta_1(x) \\ \vdots & \ddots & \vdots & \vdots \\ \sigma_{1,n}(x) & \cdots & \sigma_{n,n}(x) & n\theta_n(x) \\ W_1(x) & \cdots & W_n(x) & 0 \end{bmatrix}, \tag{C.1c}$$

so that (6) can be written as

$$\mu(x)\mathbf{k}_x(x,\xi) - \mathbf{L}(\xi)\mathbf{k}_\xi(x,\xi) = \mathbf{L}'(\xi)\mathbf{k}(x,\xi) + \mathbf{S}(\xi)\mathbf{k}(x,\xi). \tag{C.2}$$

The linear transform is given by $\mathcal{F} = \text{diag}(\mathcal{F}_n, 1)$, where $\mathcal{F}_n\mathbf{e}_\ell = \chi_{((\ell-1)/n,\ell/n]}$ with $\chi_{((\ell-1)/n,\ell/n]}$ being the indicator function of the interval $((\ell-1)/n, \ell/n]$ and $(\mathbf{e}_\ell)_{\ell=1}^n$ being the Euclidean basis of $\mathbb{R}^n$. Thus, the transform maps any $\mathbf{b} = (b_i)_{i=1}^{n+1} \in \mathbb{R}^{n+1}$ into $L^2([0,1];\mathbb{R}) \times \mathbb{R}$ as

$$\mathcal{F}\mathbf{b} = \begin{bmatrix} \sum_{i=1}^n b_i\chi_{((i-1)/n,i/n]} \\ b_{n+1}. \end{bmatrix}. \tag{C.3}$$

For any $g \in L^2([0,1];\mathbb{R})$, the adjoint $\mathcal{F}_n^*$ satisfies

$$\langle \mathcal{F}_n\mathbf{e}_\ell, g\rangle_{L^2([0,1];\mathbb{R})} = \int_{(\ell-1)/n}^{\ell/n} g(y)dy = \frac{1}{n}\langle \mathbf{e}_\ell, \mathcal{F}_n^* g\rangle_{\mathbb{R}^n}, \tag{C.4}$$

that is, $\mathcal{F}_n^*$ is given by

$$\mathcal{F}_n^* g = \left(n\int_{(i-1)/n}^{i/n} g(y)dy\right)_{i=1}^n, \tag{C.5}$$

where each component is the mean value of g over the interval $[(i-1)/n, i/n]$. Thus, $\mathcal{F}$ has the adjoint $\mathcal{F}^* = \text{diag}\,(\mathcal{F}_n^*, 1)$, which additionally satisfies $\mathcal{F}^*\mathcal{F} = I_{n+1}$, i.e., $\mathcal{F}$ (and $\mathcal{F}_n$) are isometries, and thus, norm preserving from their domain to their co-domain.

Let us now transform (C.2) from $\mathbb{R}^{n+1}$ to $L^2([0,1];\mathbb{R})\times\mathbb{R}$ by applying $\mathcal{F}$ to (C.2) from the left

$$\mu(x)\mathcal{F}\mathbf{k}_x(x,\xi)-\mathcal{F}\mathbf{L}(\xi)\mathcal{F}^*\mathcal{F}\mathbf{k}_\xi(x,\xi)= \mathcal{F}\mathbf{L}'(\xi)\mathcal{F}^*\mathcal{F}\mathbf{k}(x,\xi)+\mathcal{F}\mathbf{S}(\xi)\mathcal{F}^*\mathcal{F}\mathbf{k}(x,\xi), \tag{C.6}$$

where we also utilized $\mu(x)$ being scalar-valued and $\mathcal{F}^*\mathcal{F}=I_{n+1}$. Let g^n be a step function in y and r a scalar. Applying the transformations gives

$$\mathcal{F}\mathbf{k}(x,\xi)=\begin{bmatrix}K^n(x,\xi,\cdot)\\ \bar{K}^n(x,\xi)\end{bmatrix}, \tag{C.7a}$$

$$\mathcal{F}\mathbf{L}(\xi)\mathcal{F}^*\begin{bmatrix}g^n\\ r\end{bmatrix}=\begin{bmatrix}\lambda^n(\xi,\cdot)g^n(\cdot)\\ \mu(\xi)r\end{bmatrix}, \tag{C.7b}$$

$$\mathcal{F}\mathbf{S}(\xi)\mathcal{F}^*\begin{bmatrix}g^n\\ r\end{bmatrix}=\begin{bmatrix}\int_0^1\sigma^n(\xi,\eta,\cdot)g^n(\eta)d\eta & \theta^n(\xi,\cdot)r\\ \int_0^1 W^n(\xi,y)g^n(y)dy & 0\end{bmatrix}, \tag{C.7c}$$

with the functions $K^n,\lambda^n,\sigma^n,\theta^n,W^n$ defined in (17) and (18). Inserting (C.7) into (C.6) and writing the equations separately on $L^2([0,1];\mathbb{R})$ and $\mathbb{R}$ yields (11) with parameters $\lambda^n,\mu,\sigma^n,\theta^n,W^n$. Essentially, this amounts to $\left(K^n,\bar{K}^n\right)$ satisfying (11) on intervals for y of the form (18), which in turn implies satisfying (11) for almost all $y\in[0,1]$, i.e., in the L^2 sense with respect to y.

The boundary conditions (7) could be transformed into (12) with the same transformation, but it is more straightforward to check directly that $\left(K^n,\bar{K}^n\right)$ satisfies (12) for parameters $\theta^n,\lambda^n,\mu,q^n$. For any $i=1,2,\ldots,n$, we have for all $x\in[0,1]$ and $y\in((i-1)/n,i/n]$

$$K^n(x,x,y)=k^i(x,x)=\frac{\theta_i(x)}{\lambda_i(x)+\mu(x)}=\frac{\theta^n(x,y)}{\lambda^n(x,y)+\mu(x)}, \tag{C.8}$$

and thus, this boundary condition is satisfied for almost all $y\in[0,1]$. Moreover,

$$\mu(0)\bar{K}^n(x,0)=\frac{1}{n}\sum_{j=1}^{n}q_j\lambda_j(0)k^j(x,0) =\int_0^1 q^n(y)\lambda^n(0,y)K^n(x,0,y)dy, \tag{C.9}$$

which concludes that the boundary conditions (12) are satisfied. This concludes the proof.

2) Proof of Lemma 4.3: We begin by establishing some key properties of the solutions $\left(K^n,\bar{K}^n\right)$ and $(k,\bar{k})$. Firstly, it has been shown in [13, Sect. V] that, under Assumption 2.1, the kernel equations (6), (7) are well-posed, i.e., that the solution $\left(k^i\right)_{i=1}^{n+1}$ exists, is unique, and depends continuously on the parameters of (6), (7), and that $\left(k^i\right)_{i=1}^{n+1}$ is continuous on $\mathcal{T}$. Secondly, the functions $\left(K^n,\bar{K}^n\right)$ are constructed in Lemma 4.3 based on $\left(k^i\right)_{n=1}^{n+1}$, and thus, for almost all y, they exist, are unique, continuous on $\mathcal{T}$, and depend continuously on $\lambda^n,\mu,W^n,\theta^n,\sigma^n,q^n$ in the L^2 sense (in y). Thirdly, the existence and uniqueness of the solution $(k,\bar{k})$ to the kernel equations (11), (12) follows, provided that the parameters $\lambda,\mu,W,\theta,\sigma,q$ satisfy Assumption 3.1 [27, Thm 3]. Moreover, it has been shown in [27, Sect. VI] that $(k,\bar{k})$ are continuous on $\mathcal{T}$, and as a consequence of the estimates in [27, Sect. VI.C], the solution $(k,\bar{k})$ depends continuously on $\lambda,\mu,W,\theta,\sigma,q$.

Due to the continuity of $\left(K^n,\bar{K}^n\right)$ and $(k,\bar{k})$ on $\mathcal{T}$, the norms in (19) are continuous on $\mathcal{T}$, and hence, the maxima are reached at some point in $\mathcal{T}$. Thus, it remains to show that the maxima become arbitrarily small when n is sufficiently large. The remainder of the proof utilizes the well-posedness of the kernel equations (11), (12), in particular that the solutions $(k,\bar{k})$ and $\left(K^n,\bar{K}^n\right)$ depend continuously on the parameters of the respective kernel equations as we established in the beginning of the proof. First we show that, when n is sufficiently large, the parameters $\lambda^n,W^n,\theta^n,\sigma^n,q^n$ can approximate the respective continuum parameters $\lambda,W,\theta,\sigma,q$ to arbitrary accuracy in the L^2 sense. That is, for any $\varepsilon_1>0$, the following estimates are satisfied for any sufficiently large n

$$\max_{x\in[0,1]}\|\lambda(x,\cdot)-\lambda^n(x,\cdot)\|_{L^2([0,1];\mathbb{R})}\le\varepsilon_1, \tag{C.10a}$$

$$\max_{x\in[0,1]}\|\sigma(x,\cdot,\cdot)-\sigma^n(x,\cdot,\cdot)\|_{L^2([0,1]^2;\mathbb{R})}\le\varepsilon_1, \tag{C.10b}$$

$$\max_{x\in[0,1]}\|\theta(x,\cdot)-\theta^n(x,\cdot)\|_{L^2([0,1];\mathbb{R})}\le\varepsilon_1, \tag{C.10c}$$

$$\max_{x\in[0,1]}\|W(x,\cdot)-W^n(x,\cdot)\|_{L^2([0,1];\mathbb{R})}\le\varepsilon_1, \tag{C.10d}$$

$$\|q-q^n\|_{L^2([0,1];\mathbb{R})}\le\varepsilon_1. \tag{C.10e}$$

Existence of continuous functions $\lambda,W,\theta,\sigma,q$ satisfying (13) and Assumption 3.1 can be guaranteed by construction (see, e.g., Footnote 4). Moreover, the functions $\lambda^n,W^n,\theta^n,\sigma^n,q^n$ are continuous in x by construction and Assumption 2.1, so that the maxima in (C.10) are reached at some points $x\in[0,1]$. As the functions compared in (C.10) match for all $x\in[0,1]$ at the points $y,\eta=1/n,2/n,\ldots,1$, the differences of the functions can be made arbitrarily small in the sense of (C.10) with n being sufficiently large, e.g., based on the fact that step functions are dense in the L^2 function space [38, Sect. 1.3.5].

Finally, due to the well-posedness of the kernel equations, the solutions compared in (19) depend continuously on the parameters compared in (C.10). Thus, as ε_1 tends to zero in (C.10), the difference of the solutions $(k,\bar{k})$ and $\left(K^n,\bar{K}^n\right)$ converges to zero in a certain sense. More precisely, the convergence is exactly in the sense stated in (19), as the parameter functions converge uniformly in x by (C.10), and ξ only appears in place of x in the kernel equations. Thus, the convergence of the solutions is uniform in both x and ξ on $\mathcal{T}$, and hence, for any $\delta>0$, the estimates (19) are satisfied for any sufficiently large n.

3) Proof of Lemma 4.5: Transform the functions $\left(\widetilde{k}^i\right)_{i=1}^{n}$ from (16) into a step function in y as

$$\widetilde{K}^n(x,\xi,y)=\widetilde{k}^i(x,\xi),\quad y\in((i-1)/n,i/n], \tag{C.11}$$

for all $0\le\xi\le x\le 1$ and piecewise in y for $i=1,2,\ldots,n$. By (C.11) and (15), we have $\widetilde{K}^n(x,\xi,\cdot)=\mathcal{F}_n\mathcal{F}_n^*k(x,\xi,\cdot)$ ($\mathcal{F}_n$ was introduced in the proof of Lemma 4.2), which is the mean value approximation of $k(x,\xi,\cdot)$ for all $0 \le \xi \le x \le 1$. By [38, Sect. 1.6], the mean-value approximation becomes arbitrarily accurate for sufficiently large n, and thus, for any $\varepsilon > 0$, there exists some $n_\varepsilon \in \mathbb{N}$ such that

$$\max_{(x,\xi)\in\mathcal{T}} \|k(x,\xi,\cdot) - \widetilde{K}^n(x,\xi,\cdot)\|_{L^2([0,1];\mathbb{R})} \le \varepsilon, \qquad \text{(C.12)}$$

for any $n \ge n_\varepsilon$. Combining this with the estimates of Lemma 4.3 and using the triangle inequality, we have for any $n \ge \max\{n_\delta, n_\varepsilon\}$

$$\begin{aligned}&\max_{(x,\xi)\in\mathcal{T}} \|K^n(x,\xi,\cdot) - \widetilde{K}^n(x,\xi,\cdot)\|_{L^2([0,1];\mathbb{R})}\\ &\le \max_{(x,\xi)\in\mathcal{T}} \|K^n(x,\xi,\cdot) - k(x,\xi,\cdot)\|_{L^2([0,1];\mathbb{R})}\\ &\quad + \max_{(x,\xi)\in\mathcal{T}} \|k(x,\xi,\cdot) - \widetilde{K}^n(x,\xi,\cdot)\|_{L^2([0,1];\mathbb{R})}\\ &\le \delta + \varepsilon, \end{aligned} \qquad \text{(C.13)}$$

where both δ and ε can be made arbitrarily small by increasing n by Lemma 4.3 and (C.12), respectively. As the estimate is uniform on $\mathcal{T}$, it particularly applies on $x = 1$.

Moreover, the step functions $\widetilde{K}^n$ and K^n constructed in (C.11) and (18), respectively, are obtained through applying the isometric transform $\mathcal{F}_n$ to $\left(\widetilde{k}^i\right)_{i=1}^n$ and $\left(k^i\right)_{i=1}^n$, respectively. Thus, the estimate (C.13) also holds for the vector-valued functions, i.e.,

$$\max_{(x,\xi)\in\mathcal{T}} \frac{1}{\sqrt{n}} \left\| \left(k^i(x,\xi)\right)_{i=1}^n - \left(\widetilde{k}^i(x,\xi)\right)_{i=1}^n \right\|_{\mathbb{R}^n} \le \delta + \varepsilon. \qquad \text{(C.14)}$$

In addition, from (19) in Lemma 4.3 we already have

$$\max_{(x,\xi)\in\mathcal{T}} \left| k^{n+1}(x,\xi) - \widetilde{k}^{n+1}(x,\xi) \right| \le \delta. \qquad \text{(C.15)}$$

Now, setting $\Delta k^i = \widetilde{k}^i - k^i$ for $i = 1, 2, \ldots, n+1$, we have written (16) as (20), where the error term can be estimated using (C.14), (C.15), triangle inequality and Cauchy-Schwartz inequality as

$$\int_0^1 \left(\frac{1}{n} \sum_{i=1}^n \Delta k^i(1,\xi) u^i(t,\xi) + \Delta k^{n+1}(1,\xi) v(t,\xi) \right) d\xi \le (2\delta + \varepsilon) \left\| \begin{pmatrix} \mathbf{u}(t,\cdot) \\ v(t,\cdot) \end{pmatrix} \right\|_E, \qquad \text{(C.16)}$$

where δ and ε become arbitrarily small when n is sufficiently large.

4) Proof of Theorem 4.1 using a Lyapunov functional: By following [13, Lem. 3.1], we construct the Lyapunov functional with parameters $p, \delta_1 > 0$

$$V(t) = \int_0^1 p e^{-\delta_1 x} \frac{1}{n} \sum_{i=1}^n \frac{\alpha_i^2(t,x)}{\lambda_i(x)} dx + \int_0^1 \frac{1+x}{\mu(x)} \beta(t,x)^2 dx, \qquad \text{(C.17)}$$

where $\alpha_i(t,x) = u_i(t,x)$ for $i = 1, \ldots, n$ and

$$\beta(t,x) = v(t,x) - \int_0^x \frac{1}{n} \sum_{i=1}^n k^i(x,\xi) u^i(t,\xi) d\xi - \int_0^x k^{n+1}(x,\xi) v(t,\xi) d\xi, \qquad \text{(C.18)}$$

are the states of the target system after the exact backstepping transformation. The dynamics of the target system is of the form [13, Sect. III.A]

$$\begin{aligned}\alpha_t^i(t,x) + \lambda_i(x)\alpha_x^i(t,x) = {}& \frac{1}{n}\sum_{j=1}^n \sigma_{i,j}(x)\alpha^j(t,x) + W_i(x)\beta(t,x)\\ &+ \frac{1}{n}\sum_{j=1}^n \int_0^x c_{i,j}(x,\xi)\alpha^j(t,\xi)d\xi + \int_0^x \kappa_i(x,\xi)\beta(t,\xi)d\xi,\end{aligned} \qquad \text{(C.19a)}$$

$$\beta_t(t,x) - \mu(x)\beta_x(t,x) = 0, \qquad \text{(C.19b)}$$

with boundary conditions $\alpha^i(t,0) = q_i\beta(t,0)$ for all $i = 1, 2, \ldots, n$, where $c_{i,j}, \kappa_i$ are continuous on $\mathcal{T}$[11]. Employing the approximate control law (20), the boundary condition for β at $x = 1$ is

$$\begin{aligned}\beta(t,1) &= \int_0^1 \frac{1}{n}\sum_{i=1}^n \Delta k^i(1,\xi) u^i(t,\xi) d\xi + \int_0^1 \Delta k^{n+1}(1,\xi) v(t,\xi) d\xi\\ &= \left\langle \begin{pmatrix} \Delta\mathbf{k}(1,\cdot) \\ \Delta k^{n+1}(1,\cdot) \end{pmatrix}, \begin{pmatrix} \mathbf{u}(t,\cdot) \\ v(t,\cdot) \end{pmatrix} \right\rangle_E,\end{aligned} \qquad \text{(C.20)}$$

which also needs to be taken into account in the Lyapunov-based analysis.

Computing $\dot{V}(t)$ and integrating by parts yields

$$\begin{aligned}\dot{V}(t) = {}& \left[-p e^{-\delta_1 x} \frac{1}{n} \|\boldsymbol{\alpha}(t,x)\|_{\mathbb{R}^n}^2 + (1+x)\beta(t,x)^2 \right]_0^1\\ &- \int_0^1 \left(\delta_1 p e^{-\delta_1 x} \frac{1}{n} \|\boldsymbol{\alpha}(t,x)\|_{\mathbb{R}^n}^2 + \beta(t,x)^2 \right) dx\\ &+ \int_0^1 p e^{-\delta_1 x} \frac{1}{n} \boldsymbol{\alpha}(t,x)^T \boldsymbol{\lambda}^{-1}(x) \frac{\boldsymbol{\sigma}(x)}{n} \boldsymbol{\alpha}(t,x) dx\end{aligned}$$

[11] Under the exact backstepping controller, (C.19) would be accompanied with boundary condition $\beta(t,1) = 0$.

$$+ 2\int_0^1\int_0^x pe^{-\delta_1 x}\frac{1}{n}\boldsymbol{\alpha}(t,x)^T\boldsymbol{\lambda}^{-1}(x)\frac{\mathbf{c}(x,\xi)}{n}\boldsymbol{\alpha}(t,\xi)d\xi dx$$
$$+ 2\int_0^1 pe^{-\delta_1 x}\frac{1}{n}\boldsymbol{\alpha}(t,x)^T\boldsymbol{\lambda}^{-1}(x)\mathbf{W}(x)\beta(t,x)dx$$
$$+ 2\int_0^1\int_0^x pe^{-\delta_1 x}\frac{1}{n}\boldsymbol{\alpha}(t,x)^T\boldsymbol{\lambda}^{-1}(x)\boldsymbol{\kappa}(x,\xi)\beta(t,\xi)d\xi dx, \tag{C.21}$$

where we denote $\boldsymbol{\alpha} = (\alpha_i)_{i=1}^n, \mathbf{W} = (W_i)_{i=1}^n, \boldsymbol{\kappa} = (\kappa_i)_{i=1}^n$ and $\boldsymbol{\lambda} = \mathrm{diag}(\lambda_i)_{i=1}^n, \boldsymbol{\sigma} = (\sigma_{i,j})_{i,j=1}^n, \mathbf{c} = (c_{i,j})_{i,j=1}^n$. Since all the (individual components of the) parameters are continuous, they are also uniformly bounded on compact sets, and hence, there exist some $M_\sigma, M_W, M_c, M_\kappa > 0$ such that

$$\max_{x\in[0,1]}\frac{\|\boldsymbol{\sigma}(x)\|_\infty}{n} \le M_\sigma, \tag{C.22a}$$
$$\max_{x\in[0,1]}\|\mathbf{W}(x)\|_\infty \le M_W, \tag{C.22b}$$
$$\max_{(x,\xi)\in\mathcal{T}}\frac{\|\mathbf{c}(x,\xi)\|_\infty}{n} \le M_c, \tag{C.22c}$$
$$\max_{(x,\xi)\in\mathcal{T}}\|\boldsymbol{\kappa}(x,\xi)\|_\infty \le M_\kappa. \tag{C.22d}$$

Moreover, since $\boldsymbol{\lambda}(x)$ is diagonal and uniformly bounded away from zero by Assumption 2.1, there exists some $M_\lambda > 0$ such that $\max_{x\in[0,1]}\|\boldsymbol{\lambda}^{-1}(x)\|_\infty \le M_\lambda$. Thus, we eventually get

$$\dot V(t) \le -\left(1 - p\frac{1}{n}\sum_{i=1}^n q_i^2\right)\beta(t,0)^2 + 2\beta(t,1)^2$$
$$-\int_0^1\left(1 - pM_\lambda M_W - \frac{pM_\lambda M_\kappa}{\delta_1}\right)\beta(t,x)^2dx$$
$$-\int_0^1 pe^{-\delta_1 x}(\delta_1 - \widetilde{M})\frac{1}{n}\|\boldsymbol{\alpha}(t,x)\|^2_{\mathbb{R}^n}dx, \tag{C.23}$$

where $\widetilde{M} = M_\lambda M_\sigma + 2\frac{M_\lambda M_c}{\delta_1} + M_\lambda M_W + \frac{M_\lambda M_\kappa}{\delta_1}$[12]. We have the following estimate from (C.20) and (C.16)

$$2\beta(t,1)^2 \le 2(2\delta+\varepsilon)^2\left\|\begin{pmatrix}\mathbf{u}(t,\cdot)\\ v(t,\cdot)\end{pmatrix}\right\|_E^2, \tag{C.24}$$

where $u^i = \alpha^i$ for all $i = 1,2,\ldots,n$. Moreover, there exist inverse kernels $\left(l^i\right)_{i=1}^{n+1}$ such that [13, Sect. III.A.3]

$$v(t,x) = \beta(t,x) + \left\langle\begin{pmatrix}\mathbf{l}(x,\cdot)\\ l^{n+1}(x,\cdot)\end{pmatrix},\begin{pmatrix}\boldsymbol{\alpha}(t,\cdot)\\ \beta(t,\cdot)\end{pmatrix}\right\rangle_E, \tag{C.25}$$

where $\left(l^i\right)_{i=1}^{n+1}$ are continuous on $\mathcal{T}$, and hence, also uniformly bounded. Thus, there exists some $M_l > 0$ such that

$$\max_{(x,\xi)\in\mathcal{T}}\max_{i\in\{1,2,\ldots,n+1\}}\left|l^i(x,\xi)\right| \le M_l. \tag{C.26}$$

By Jensen's inequality we thus have

$$\left\|\begin{pmatrix}\mathbf{u}(t,\cdot)\\ v(t,\cdot)\end{pmatrix}\right\|_E^2 \le (1+M_l)^2\left\|\begin{pmatrix}\boldsymbol{\alpha}(t,\cdot)\\ \beta(t,\cdot)\end{pmatrix}\right\|_E^2, \tag{C.27}$$

[12] If $\beta(t,1) = 0$, under the exact controller, then $\dot V(t)$ is negative definite for some sufficiently small $p > 0$ and sufficiently large $\delta_1 > 0$.

which finally yields

$$2\beta(t,1)^2 \le 2(2\delta+\varepsilon)^2(1+M_l)^2\left\|\begin{pmatrix}\boldsymbol{\alpha}(t,\cdot)\\ \beta(t,\cdot)\end{pmatrix}\right\|_E^2. \tag{C.28}$$

Relation (C.28) implies that when δ and ε are sufficiently small, $\dot V(t)$ in (C.23) can be made negative definite, with a proper choice of p, δ_1, despite the perturbation acting on $\beta(t,1)$.

To complete the proof, we note that $V(t)$ in (C.17) corresponds to the weighted inner product $V(t) = \left\langle\begin{pmatrix}\boldsymbol{\alpha}(t,\cdot)\\ \beta(t,\cdot)\end{pmatrix},\mathbf{P}(\cdot)\begin{pmatrix}\boldsymbol{\alpha}(t,\cdot)\\ \beta(t,\cdot)\end{pmatrix}\right\rangle_E$, where $\mathbf{P}(x) = \mathrm{diag}\left(pe^{-\delta_1 x}\boldsymbol{\lambda}^{-1}(x), \frac{1+x}{\mu(x)}\right) > 0$ for all $x \in [0,1]$, by which there exists some $m_V, M_V > 0$ such that

$$m_V\left\|\begin{pmatrix}\boldsymbol{\alpha}(t,\cdot)\\ \beta(t,\cdot)\end{pmatrix}\right\|_E^2 \le V(t) \le M_V\left\|\begin{pmatrix}\boldsymbol{\alpha}(t,\cdot)\\ \beta(t,\cdot)\end{pmatrix}\right\|_E^2. \tag{C.29}$$

Moreover, from (C.23) and (C.28) we get $\dot V(t) \le -c_V\left\|\begin{pmatrix}\boldsymbol{\alpha}(t,\cdot)\\ \beta(t,\cdot)\end{pmatrix}\right\|_E^2$ with $c_V = \min\left\{1 - pM_\lambda M_W - \frac{pM_\lambda M_\kappa}{\delta_1}, pe^{-\delta_1}\left(\delta_1 - \widetilde{M}\right)\right\} - 2(2\delta+\varepsilon)^2(1+M_l^2)$, which can be made positive for a large δ_1 and small p, δ, ε. Thus, we have

$$\left\|\begin{pmatrix}\boldsymbol{\alpha}(t,\cdot)\\ \beta(t,\cdot)\end{pmatrix}\right\|_E^2 \le \frac{m_V}{M_V}\left\|\begin{pmatrix}\boldsymbol{\alpha}(0,\cdot)\\ \beta(0,\cdot)\end{pmatrix}\right\|_E^2\exp\left(-\frac{c_V}{M_V}t\right). \tag{C.30}$$

Finally, using (C.27) and an analogous estimate for the forward transform (C.18) as $\|\left(\begin{smallmatrix}\boldsymbol{\alpha}\\ \beta\end{smallmatrix}\right)\|_E \le (1+M_k)\|\left(\begin{smallmatrix}\boldsymbol{u}\\ v\end{smallmatrix}\right)\|_E$, for some $M_k > 0$ such that $\max_{(x,\xi)\in\mathcal{T}}\max_{i\in\{1,2,\ldots,n+1\}}\left|k^i(x,\xi)\right| \le M_k$, we obtain

$$\left\|\begin{pmatrix}\mathbf{u}(t,\cdot)\\ v(t,\cdot)\end{pmatrix}\right\|_E^2 \le \widetilde{M}_V\left\|\begin{pmatrix}\mathbf{u}(0,\cdot)\\ v(0,\cdot)\end{pmatrix}\right\|_E^2\exp\left(-\frac{c_V}{M_V}t\right), \tag{C.31}$$

where $\widetilde{M}_V = (1+M_l)^2\frac{m_V}{M_V}(1+M_k)^2$, which completes the proof.

Remark C.1: Technically, the Lyapunov-based arguments presented apply to classical solutions, the existence of which can be guaranteed for any initial conditions $u_0^i, v_0 \in H^1([0,1];\mathbb{R})$ that satisfy the compatibility conditions $u_0^i(0) = q_i v_0(0)$ and $v_0(1) = \frac{1}{n}\sum_{i=1}^n r_i u_0^i(1) + U(0)$ [31, Prop. 10.1.8]. However, as noted in [7, Sect. 2.1.3], for any weak solution there exists a sequence of classical solutions which converges to the weak solution in E, and hence, the decay estimate (C.31) also applies to weak solutions.

5) Proof of Proposition 4.7: Based on (11), (12), the difference variables $\Delta k = k - K^n$ and $\Delta\bar k = \bar k - \bar K^n$ satisfy the kernel equations

$$\mu(x)\Delta k_x(x,\xi,y) - \lambda(\xi,y)\Delta k_\xi(x,\xi,y) - \Delta k(x,\xi,y)\lambda_\xi(\xi,y) = \theta(\xi,y)\Delta\bar k(x,\xi) + \Delta\lambda_\xi(\xi,y)K^n(x,\xi,y)$$
$$+ \int_0^1\sigma(\xi,\eta,y)\Delta k(x,\xi,\eta)d\eta + \Delta\lambda(\xi,y)K_\xi^n(x,\xi,y)$$
$$+ \int_0^1\Delta\sigma(\xi,\eta,y)K^n(x,\xi,\eta)d\eta + \Delta\theta(\xi,y)\bar K^n(x,\xi), \tag{C.32a}$$

$$\mu(x)\Delta\bar{k}_x(x,\xi)+\mu(\xi)\Delta\bar{k}_\xi(x,\xi)+\mu'(\xi)\Delta\bar{k}(x,\xi)= \int_0^1 \left(W(\xi,y)\Delta k(x,\xi,y)+\Delta W(\xi,y)K^n(x,\xi,y)\right)dy, \tag{C.32b}$$

where we denote $\Delta\lambda=\lambda-\lambda^n, \Delta\theta=\theta-\theta^n, \Delta\sigma=\sigma-\sigma^n, \Delta W=W-W^n$, with boundary conditions

$$\Delta k(x,x,y)=-\frac{\Delta\theta(x,y)+\Delta\lambda(x,y)K^n(x,x,y)}{\Delta\lambda(x,y)+\mu(x)}, \tag{C.33a}$$

$$\mu(0)\Delta\bar{k}(x,0)=\int_0^1 q(y)\lambda(0,y)\Delta k(x,0,y)dy + \int_0^1 \Delta b(y)K^n(x,0,y)dy, \tag{C.33b}$$

where we denote $\Delta b(y)=\Delta q(y)\lambda^n(0,y)+\Delta q(y)\Delta\lambda(0,y)+q^n(y)\Delta\lambda(0,y)$. The kernel equations (C.32), (C.33) are essentially of the same form as (11), (12) with some additional terms due to the parameter approximation errors. Note that $(K^n,\bar{K}^n)$ is treated as a parameter and from Lemma 4.2 it follows that it can be estimated (i.e., bounded in norm) by [13, Prop. 5.6], where the L^2 norms (in y) of the step function parameters can be bounded independently of n, in view of (13), (17), by the L^∞ norm of the respective continuum parameters. In fact, we can take in (23a), (23b) $\bar{M}_1=M$ and[13]

$$\bar{\phi}=M_q\frac{\max_{x\in[0,1]}\|\theta(x,\cdot)\|_{L^\infty([0,1];\mathbb{R})}}{m_\lambda+m_\mu}. \tag{C.34}$$

In the limiting case $n\to\infty$, we have $K^\infty=k$ and $\bar{K}^\infty=\bar{k}$ by (19), so that the same estimates remain valid by [27, Sect. VI.C].

A similar bound (23c) for K^n_ξ can be derived by differentiating with respect to x and ξ equations (6), (7), which results in kernel equations for $\left(k^i_x,k^i_\xi\right)_{i=1}^{n+1}$ that are of the same form as (6), (7) with some additional terms due to differentiation (see, e.g., [36, App. A.4] for a 2×2 case). Due to the additional smoothness assumptions on the parameters, differentiating both sides of (13) and (17) with respect to x gives the respective relations for the derivatives. This allows to employ Lemma 4.2 for k^i_x and k^i_ξ with the respective (derivatives of the) parameters. Employing similar arguments as for estimating K^n and $\bar{K}^n$, analogously to [13, Prop. 5.6] (and [27, Sect. VI.C] in the limiting case $n\to\infty$), we can bound K^n_ξ independently of n with (23c) by choosing

$$\bar{M}_1'=\bar{M}_1+\frac{M_q}{m_\lambda}(M_\mu'+M_\lambda')+\frac{M_\mu'}{m_\mu}, \tag{C.35}$$

$$\begin{aligned}\bar{\phi}'=&\,M_qM_B+2M_q\bar{\phi}e^{\bar{M}_1}\Bigg(\max_{x\in[0,1]}\|\lambda_{xx}(x,\cdot)\|_{L^\infty([0,1];\mathbb{R})}\\ &+\max_{x\in[0,1]}\|\theta_x(x,\cdot)\|_{L^\infty([0,1];\mathbb{R})}\\ &+\max_{x\in[0,1]}\left\|\int_0^1\sigma_x(x,\cdot,\eta)d\eta\right\|_{L^\infty([0,1];\mathbb{R})}\Bigg)\\ &+\frac{M_\mu'+\max_{x\in[0,1]}\|W(x,\cdot)\|_{L^\infty([0,1];\mathbb{R})}}{m_\mu}\bar{\phi}e^{\bar{M}_1}\\ &+2\frac{\max_{x\in[0,1]}|\mu''(x)|+\max_{x\in[0,1]}\|W_x(x,\cdot)\|_{L^\infty([0,1];\mathbb{R})}}{m_\mu}\bar{\phi}e^{\bar{M}_1},\end{aligned} \tag{C.36}$$

where

$$\begin{aligned}M_B=&\,\frac{M_\mu+M_\lambda}{(m_\mu+m_\lambda)^3}\Bigg(\max_{x\in[0,1]}\|\theta(x,\cdot)\|_{L^\infty([0,1];\mathbb{R})}(M_\mu'+M_\lambda')\\ &+\max_{x\in[0,1]}\|\theta_x(x,\cdot)\|_{L^\infty([0,1];\mathbb{R})}(M_\mu+M_\lambda)\Bigg)\\ &+\Bigg(M_\lambda'+\max_{x\in[0,1]}\|\theta(x,\cdot)\|_{L^\infty([0,1];\mathbb{R})}\\ &+\max_{x\in[0,1]}\left\|\int_0^1\sigma(x,\cdot,\eta)d\eta\right\|_{L^\infty([0,1];\mathbb{R})}\Bigg)\frac{\bar{\phi}e^{\bar{M}_1}}{m_\mu+m_\lambda},\end{aligned} \tag{C.37}$$

$$M_\lambda=\max_{x\in[0,1]}\|\lambda(x,\cdot)\|_{L^\infty([0,1];\mathbb{R})},\quad M_\mu=\max_{x\in[0,1]}\mu(x). \tag{C.38}$$

Finally, the estimate (21) follows after finding an upper bound for the solution to (C.32), (C.33), which is achieved by employing the method of successive approximations similarly to [27, Sect. VI.C]. In particular, the characteristic curves of (C.32) are the same as in [27, Sect. VI], so that we can transform (C.32), (C.33) into integral equations along the characteristic curves and employ the estimates (C.10) with $\varepsilon_1=M_L/n$ due to the Lipschitz-continuity of the continuum parameters.[14] Note that, in addition to the L^2 norm, such estimates (C.10) hold in the L^∞ norm as well (this is needed for estimating Δb). Moreover, as the characteristic curves are monotonic due to $\lambda,\mu>0$ by Assumption 3.1, due to the geometry of $\mathcal{T}$ the lengths of the characteristic curves are bounded from above by 2, which amounts to the numerical coefficients appearing in (21). The rest of the proof relies on the same arguments employed in [27]. Specifically, by initiating the sequence of successive approximations (see [27, (109), (110)]) with zero, the first step involves integrating

[13]Note that the n coefficients appearing in the proof of [13, Prop. 5.6] are canceled out here due to scaling of the respective sums in (6), (7) by $1/n$.

[14]This follows by (13), (17), and Lipschitz continuity, as for any $y\in((i-1)/n,i/n]$ with $i=1,\dots,n$ arbitrary, we have, e.g., for q,

$$|q(y)-q^n(y)|=\left|q(y)-q\left(\frac{i}{n}\right)\right|\le M_L\left|y-\frac{i}{n}\right|\le\frac{M_L}{n}. \tag{C.39}$$

the additive terms (i.e., those not involving $(\Delta k, \Delta\bar{k})$) of (C.32) along the characteristic curves and plugging in the boundary conditions, where the additive terms depend on the parameter approximation errors. Thereafter, these additive terms cancel out when the difference of subsequent successive approximations is considered, and hence, the convergence of the sequence of successive approximations for $(\Delta k, \Delta\bar{k})$ follows after exactly the same induction arguments as in [27, Sect. VI.C], resulting in the estimate $\delta = M_\delta/n$ with M_δ given in (21).

6) Proof of Theorem 6.1: Firstly, we note that (8), (9) is well-posed on $E_c = L^2([0,1]; L^2([0,1];\mathbb{R})) \times L^2([0,1];\mathbb{R})$ under Assumption 3.1 as shown in Proposition B.1 in Appendix B. That is, for any initial conditions $u_0 \in L^2([0,1]; L^2([0,1];\mathbb{R})), v_0 \in L^2([0,1];\mathbb{R})$ and input $U \in L^2_{\text{loc}}([0,+\infty);\mathbb{R})$, the solution (u,v) is well-defined, unique, continuous in time, and depends continuously on the data of the problem on any compact interval $t \in [0,T]$, for any given $T > 0$. In particular, there exist families of bounded linear operators $\mathbb{T}_t, \Phi_t$ for $t \geq 0$, depending continuously on the parameters $\lambda, \mu, \sigma, \theta, W, q, r$, such that the solution to (8), (9) is given by [31, Prop. 4.2.5]

$$\begin{pmatrix} u(t) \\ v(t) \end{pmatrix} = \mathbb{T}_t \begin{pmatrix} u_0 \\ v_0 \end{pmatrix} + \Phi_t U, \tag{C.40}$$

which satisfies $\begin{pmatrix} u \\ v \end{pmatrix} \in C([0,+\infty); E_c)$. The well-posedness and regularity of solutions to (3), (4) have already been established in Proposition A.1 in Appendix A and Remark 2.2.

Secondly, based on the parameters $\lambda_i, W_i, \theta_i, \sigma_{i,j}, q_i, r_i$ for $i,j = 1,2,\ldots,n$ of (3), (4), we can construct the step functions $\lambda^n, \sigma^n, \theta^n, W^n, q^n$ as in (17) and r^n analogously to q^n such that they satisfy (C.10) for any $\varepsilon_1 > 0$ when n is sufficiently large. Moreover, we can transform the solution to (3), (4) into a step function (in y) by applying the transform $\mathcal{F}$ introduced in the proof of Lemma 4.2, i.e.,

$$\begin{pmatrix} u^n(t,x,\cdot) \\ v^n(t,x) \end{pmatrix} = \mathcal{F} \begin{pmatrix} \mathbf{u}(t,x) \\ v(t,x) \end{pmatrix}. \tag{C.41}$$

That is, u^n is defined piecewise in y, for $i = 1,2,\ldots,n$, as $u^n(t,x,y) = u^i(t,x)$, $y \in ((i-1)/n, i/n]$, pointwise for all $t \in [0,T]$ and almost all $x \in [0,1]$. Then (u^n, v^n) is the solution to (8), (9) for parameters $\lambda^n, \mu, \sigma^n, \theta^n, W^n, q^n, r^n$, input U, and initial conditions $v_0, u_0^n(x,\cdot) = \mathcal{F}_n \mathbf{u}_0(x)$. This can be verified by applying the transform $\mathcal{F}$ to (3), (4) (from the left), for each $t \geq 0$ and almost all $x \in [0,1]$, which results in (u^n, v^n) satisfying (8), (9) for the stated parameters, initial conditions, and input. (This follows in a similar manner with the respective part of the proof of Lemma 4.2.) As (3), (4) is well-posed, the transformed solution (3), (4) is the well-posed solution to the transformed (by $\mathcal{F}$) PDE system. In particular, there exist families of operators $\mathbb{T}_t^n, \Phi_t^n$ for $t \geq 0$, depending continuously on the parameters $\lambda^n, \mu, \sigma^n, \theta^n, W^n, q^n, r^n$, such that the solution to (8), (9) for these parameters is given by

$$\begin{pmatrix} u^n(t) \\ v^n(t) \end{pmatrix} = \mathbb{T}_t^n \begin{pmatrix} u_0^n \\ v_0 \end{pmatrix} + \Phi_t^n U, \tag{C.42}$$

which satisfies $\begin{pmatrix} u^n \\ v^n \end{pmatrix} \in C([0,+\infty); E_c)$.

Thirdly, consider the difference of the solutions (to (8), (9)) (C.40) and (C.42), under the respective parameters and initial conditions, and the same inputs on the interval $t \in [0,T]$. We get, for each $t \in [0,T]$,

$$\begin{aligned} \left\| \begin{pmatrix} u(t) \\ v(t) \end{pmatrix} - \begin{pmatrix} u^n(t) \\ v^n(t) \end{pmatrix} \right\|_{E_c} &\leq \left\| (\mathbb{T}_t - \mathbb{T}_t^n) \begin{pmatrix} u_0^n \\ v_0 \end{pmatrix} \right\|_{E_c} \\ &\quad + \|\mathbb{T}_t\|_{\mathcal{L}(E_c)} \left\| \begin{pmatrix} u_0 \\ v_0 \end{pmatrix} - \begin{pmatrix} u_0^n \\ v_0 \end{pmatrix} \right\|_{E_c} \\ &\quad + \|(\Phi_t - \Phi_t^n) U\|_{E_c} \\ &\leq \delta_2 + \varepsilon_2 + \delta_3, \end{aligned} \tag{C.43}$$

where, for any given T, u_0, v_0, and U, the constants $\delta_2, \varepsilon_2, \delta_3$ can be made arbitrarily small by taking n sufficiently large. That is, δ_2 and δ_3[15] become small due to the solution to (8), (9) depending continuously on the parameters, initial conditions, and input of the problem, i.e., δ_2 and δ_3 depend continuously on ε_1 in (C.10) such that $\delta_2, \delta_3 \to 0$ as $\varepsilon_1 \to 0$. The second term ε_2 becomes small as $\|\mathbb{T}_t\|_{\mathcal{L}(E_c)}$ is uniformly bounded on $t \in [0,T]$ by Proposition B.1; while the difference $\|u_0 - u_0^n\|_{L^2([0,1]^2;\mathbb{R})}$ can be made arbitrarily small due to (28) and $u_0^n(x,\cdot) = \mathcal{F}_n \mathbf{u}_0(x)$, analogously to (C.10).

Finally, set $\widetilde{\mathbf{u}}(t,x) = \mathcal{F}_n^* u(t,x,\cdot)$ and $\widetilde{v} = v$ for all $t \in [0,T]$ and almost all $x \in [0,1]$, i.e., each component of $\widetilde{\mathbf{u}}$ is

$$\widetilde{u}^i(t,x) = n \int_{(i-1)/n}^{i/n} u(t,x,y)dy, \tag{C.44}$$

which is the mean value of $u(t,x,\cdot)$ over an interval of length $1/n$ in y. Since $\mathcal{F}$ is an isometry, we have, for each $t \in [0,T]$,

$$\begin{aligned} \left\| \begin{pmatrix} \mathbf{u}(t) \\ v(t) \end{pmatrix} - \begin{pmatrix} \widetilde{\mathbf{u}}(t) \\ \widetilde{v}(t) \end{pmatrix} \right\|_E &= \left\| \mathcal{F} \left(\begin{pmatrix} \mathbf{u}(t) \\ v(t) \end{pmatrix} - \begin{pmatrix} \widetilde{\mathbf{u}}(t) \\ \widetilde{v}(t) \end{pmatrix} \right) \right\|_{E_c} \\ &\leq \left\| \begin{pmatrix} u^n(t) \\ v^n(t) \end{pmatrix} - \begin{pmatrix} u(t) \\ v(t) \end{pmatrix} \right\|_{E_c} \\ &\quad + \left\| \begin{pmatrix} u(t) \\ v(t) \end{pmatrix} - \mathcal{F}\mathcal{F}^* \begin{pmatrix} u(t) \\ v(t) \end{pmatrix} \right\|_{E_c} \\ &\leq \delta_2 + \varepsilon_2 + \delta_3 + \varepsilon_3, \end{aligned} \tag{C.45}$$

where we used the triangle inequality (added and subtracted (u,v)), definitions (C.41) and (C.44), and (C.43). Moreover, $\varepsilon_3 > 0$ can be made arbitrarily small, as the solution (u,v) is uniformly bounded on $t \in [0,T]$ and the step function $\mathcal{F}\mathcal{F}^* \begin{pmatrix} u(t) \\ v(t) \end{pmatrix}$ can approximate $\begin{pmatrix} u(t) \\ v(t) \end{pmatrix}$ to arbitrary accuracy (for almost all $x,y \in [0,1]$, uniformly in $t \in [0,T]$) when n is sufficiently large, i.e., when the interval length $1/n$ becomes sufficiently small (by mean-value approximation, see, e.g., [38, Sect. 1.6]). Thus, the maximum of (C.45) over $t \in [0,T]$ can be made arbitrarily small by taking n sufficiently large, which yields (29).

References

[1] V. Bikia, "Non-invasive monitoring of key hemodynamical and cardiac parameters using physics-based modelling and artificial intelligence," Ph.D. dissertation, EPFL, 2021.

[2] P. Reymond, F. Merenda, F. Perren, D. Rufenacht, and N. Stergiopulos, "Validation of a one-dimensional model of the systemic arterial tree," *Am. J. Physiol. Heart Circ. Physiol.*, vol. 297, pp. H208–H222, 2009.

[15] Note that δ_2 and δ_3 are the maxima over $[0,T]$ of the respective constants satisfying (C.43) for each $t \in [0,T]$.

[3] L. Guan, C. Prieur, L. Zhang, C. Prieur, D. Georges, and P. Bellemain, "Transport effect of COVID-19 pandemic in France," *Annu. Rev. Control*, vol. 50, pp. 394–408, 2020.
[4] J. Friedrich, S. Göttlich, and M. Osztfalk, "Network models for nonlocal traffic flow," *ESAIM Math. Model. Numer. Anal.*, vol. 56, no. 1, pp. 213–235, 2022.
[5] L. Zhang, H. Luan, Y. Lu, and C. Prieur, "Boundary feedback stabilization of freeway traffic networks: ISS control and experiments," *IEEE Trans. Control Syst. Technol.*, vol. 30, pp. 997–1008, 2022.
[6] L. Tumash, C. Canudas-de-Wit, and M. L. Delle Monache, "Multi-directional continuous traffic model for large-scale urban networks," *Transportation Research Part B: Methodological*, vol. 158, pp. 374–402, 2022.
[7] G. Bastin and J.-M. Coron, *Stability and Boundary Sabilization of 1-D Hyperbolic Systems*. Birkhäuser/Springer, [Cham], 2016.
[8] J. Auriol and D. Bresch-Pietri, "Robust state-feedback stabilization of an underactuated network of interconnected $n + m$ hyperbolic PDE systems," *Automatica*, vol. 136, p. 110040, 2022.
[9] M. Krstic and A. Smyshlyaev, *Boundary Control of PDEs: A Course on Backstepping Designs*. SIAM, 2008.
[10] J. Auriol, "Output feedback stabilization of an underactuated cascade network of interconnected linear PDE systems using a backstepping approach," *Automatica*, vol. 117, p. 108964, 2020.
[11] L. Hu, F. Di Meglio, R. Vazquez, and M. Krstic, "Control of homodirectional and general heterodirectional linear coupled hyperbolic PDEs," *IEEE Trans. Automat. Control*, vol. 61, no. 11, pp. 3301–3314, 2016.
[12] J. Redaud, J. Auriol, and S.-I. Niculescu, "Output-feedback control of an underactuated network of interconnected hyperbolic PDE-ODE systems," *Syst. Control Lett.*, vol. 154, p. 104984, 2021.
[13] F. Di Meglio, R. Vazquez, and M. Krstic, "Stabilization of a system of $n+1$ coupled first-order hyperbolic linear PDEs with a single boundary input," *IEEE Trans. Automat. Control*, vol. 58, no. 12, pp. 3097–3111, 2013.
[14] T. Enderes, J. Gabriel, and J. Deutscher, "Cooperative output regulation for networks of hyperbolic systems using adaptive cooperative observers," *Automatica*, vol. 162, p. 111506, 2024.
[15] L. Paunonen and J.-P. Humaloja, "On robust regulation of PDEs: from abstract methods to PDE controllers," in *IEEE Conference on Decision and Control*, 2022, pp. 7352–7357.
[16] V. D. Blondel, J. M. Hendrickx, and J. N. Tsitsiklis, "On Krause's multi-agent consensus model with state-dependent connectivity," *IEEE Trans. Automat. Control*, vol. 54, no. 11, pp. 2586–2597, 2009.
[17] G. Ferrari-Trecate, A. Buffa, and M. Gati, "Analysis of coordinations in multi-agent systems through partial difference equations," *IEEE Trans. Automat. Control*, vol. 51, no. 6, pp. 1058–1063, 2006.
[18] T. Meurer and M. Krstic, "Finite-time multi-agent deployment: A nonlinear PDE motion planning approach," *Automatica*, vol. 37, pp. 2534–2542, 2011.
[19] D. Nikitin, C. Canudas-de-Wit, and P. Frasca, "A continuation method for large-scale modeling and control: from ODEs to PDE, a round trip," *IEEE Trans. Automat. Control*, vol. 67, pp. 5118–5133, 2022.
[20] J. Wei, E. Fridman, and K. H. Johansson, "A PDE approach to deployment of mobile agents under leader relative position measurements," *Automatica*, vol. 106, pp. 47–53, 2019.
[21] J. Qi, R. Vazquez, and M. Krstic, "Multi-agent deployment in 3-D via PDE control," *IEEE Trans. Automat. Control*, vol. 60, no. 4, pp. 891–906, 2015.
[22] P. Frihauf and M. Krstic, "Leader-enabled deployment into planar curves: A PDE-based approach," *IEEE Trans. Automat. Control*, vol. 56, pp. 1791–1806, 2011.
[23] J. Zhang, R. Vazquez, J. Qi, and M. Krstic, "Multi-agent deployment in 3-D via reaction-diffusion system with radially-varying reaction," *Automatica*, vol. 161, p. 111491, 2024.
[24] L. Bhan, Y. Shi, and M. Krstic, "Neural operators for bypassing gain and control computations in PDE backstepping," *IEEE Trans. Automat. Control*, 2024.
[25] J. Auriol, K. A. Morris, and F. Di Meglio, "Late-lumping backstepping control of partial differential equations," *Automatica*, vol. 100, pp. 247–259, 2019.
[26] R. Vazquez, G. Chen, J. Qiao, and M. Krstic, "The power series method to compute backstepping kernel gains: theory and practice," in *IEEE Conference on Decision and Control*, 2023, pp. 8162–8169.
[27] V. Alleaume and M. Krstic, "Ensembles of hyperbolic PDEs: Stabilization by backstepping," *IEEE Trans. Automat. Control*, pp. 1–16, 2024.
[28] I. Atamas, S. Dashkovskiy, and V. Slynko, "Lyapunov functions for linear hyperbolic systems," *IEEE Trans. Automat. Control*, vol. 68, pp. 6496–6508, 2023.
[29] A. Terrand-Jeanne, V. Andrieu, V. Dos Santos, and C.-Z. Xu, "Adding integral action for open-loop exponentially stable semigroups and application to boundary control of PDE systems," *IEEE Trans. Automat. Control*, vol. 65, no. 11, pp. 4481–4492, 2020.
[30] B. Jacob and H. Zwart, *Linear Port-Hamiltonian Systems on Infinite-dimensional Spaces*, ser. Operator Theory: Advances and Applications. Birkhäuser, 2012, vol. 223.
[31] M. Tucsnak and G. Weiss, *Observation and Control for Operator Semigroups*. Birkhäuser Verlag AG, 2009.
[32] R. Vazquez and M. Krstic, "Marcum Q-functions and explicit kernels for stabilization of 2×2 linear hyperbolic systems with constant coefficients," *Syst. Control Lett.*, vol. 68, pp. 33–42, 2014.
[33] J.-P. Humaloja and N. Bekiaris-Liberis, "On computation of approximate solutions to large-scale backstepping kernel equations via continuum approximation," *Syst. Control Lett.*, vol. 196, p. 105982, 2025.
[34] H. Yu and M. Krstic, *Traffic Congestion Control by PDE Backstepping*. Birkhäuser/Springer, [Cham], 2022.
[35] K.-J. Engel and R. Nagel, *One-Parameter Semigroups for Linear Evolution Equations*. Springer, 2000.
[36] J.-M. Coron, R. Vazquez, M. Krstic, and G. Bastin, "Local exponential H^2 stabilization of a 2×2 quasilinear hyperbolic system using backstepping," *SIAM J. Control Optim.*, vol. 51, no. 3, pp. 2005–2035, 2013.
[37] A. Cheng and K. A. Morris, "Well-posedness of boundary control systems," *SIAM J. Control Optim.*, vol. 42, no. 4, pp. 1244–1265, 2003.
[38] T. Tao, *An Introduction to Measure Theory*. American Mathematical Society, 2011.

Jukka-Pekka Humaloja (Member, IEEE) Received the Ph.D. degree in engineering and natural sciences from Tampere University (of Technology –2018), Finland, in 2019, where he also was a Postdoctoral Research Fellow from 2019 to 2021. From 2021 to 2023 he was a Postdoctoral Fellow with University of Alberta, Canada, and in 2024, he was a Visiting Lecturer with Aalto University, Finland. Currently he is a Postdoctoral Associate with the Technical University of Crete, Greece. His research interests include control and estimation of distributed parameter systems and large-scale systems, especially robust output regulation and model predictive control of boundary-controlled PDEs, and virtual decomposition control. He is the recipient of personal postdoctoral grants from the Jenny and Antti Wihuri Foundation (2021–2022) and the Vilho, Yrjö and Kalle Väsälä Foundation (2022–2023).

Nikolaos Bekiaris-Liberis (Senior Member, IEEE) received the Ph.D. degree in aerospace engineering from University of California, San Diego in 2013. From 2013 to 2014, he was a Post-Doctoral Researcher with University of California, Berkeley. From 2019 to 2022, he was an Assistant Professor, from 2017 to 2019, he was a Marie Sklodowska-Curie Fellow, and from 2014 to 2017, he was a Research Associate with the Technical University of Crete, Greece, where he is currently an Associate Professor with the Department of Electrical and Computer Engineering. He has authored/coauthored one book and more than 110 papers. His research interests include nonlinear delay, switched, and distributed parameter systems, and their applications to transport systems.

He serves as Associate Editor for Automatica and IEEE Transactions on Intelligent Transportation Systems. He received the Chancellor's Dissertation Medal in Engineering from University of California, San Diego in 2014 and the George N. Saridis Outstanding Research Paper Award in 2019 (from the IEEE Intelligent Transportation Systems Society). He was a recipient of a 2016 Marie Sklodowska-Curie Individual Fellowship Grant and he received a 2022 European Research Council (ERC) Consolidator Grant.